Cell

Npas4 Regulates Excitatory-Inhibitory Balance within Neural Circuits through Cell-Type-Specific Gene Programs

Ivo Spiegel,[1,3] Alan R. Mardinly,[1,2,3] Harrison W. Gabel,[1] Jeremy E. Bazinet,[1] Cameron H. Couch,[1] Christopher P. Tzeng,[1,2] David A. Harmin,[1] and Michael E. Greenberg[1,*]
[1]Department of Neurobiology, Harvard Medical School, 220 Longwood Avenue, Boston, MA 02115, USA
[2]Program in Neuroscience, Harvard Medical School, 220 Longwood Avenue, Boston, MA 02115, USA
[3]Co-first author
*Correspondence: meg@hms.harvard.edu
http://dx.doi.org/10.1016/j.cell.2014.03.058

SUMMARY

The nervous system adapts to experience by inducing a transcriptional program that controls important aspects of synaptic plasticity. Although the molecular mechanisms of experience-dependent plasticity are well characterized in excitatory neurons, the mechanisms that regulate this process in inhibitory neurons are only poorly understood. Here, we describe a transcriptional program that is induced by neuronal activity in inhibitory neurons. We find that, while neuronal activity induces expression of early-response transcription factors such as Npas4 in both excitatory and inhibitory neurons, Npas4 activates distinct programs of late-response genes in inhibitory and excitatory neurons. These late-response genes differentially regulate synaptic input to these two types of neurons, promoting inhibition onto excitatory neurons while inducing excitation onto inhibitory neurons. These findings suggest that the functional outcomes of activity-induced transcriptional responses are adapted in a cell-type-specific manner to achieve a circuit-wide homeostatic response.

INTRODUCTION

Experience-dependent synaptic plasticity underlies multiple aspects of learning and memory and is important early in life during critical periods when sensory experience is necessary for the development of cortical circuits (Hensch, 2005; Wiesel and Hubel, 1963). Research over several decades has revealed that physical changes at synapses that form on excitatory and inhibitory neurons are important for the nervous system's adaptive responses to sensory input. Though specific molecular mechanisms by which neuronal activity modifies synapses on excitatory neurons have been identified, it remains to be determined how synapses on cortical inhibitory neurons adapt to changing levels of neuronal activity. Because inhibition is critically important for experience-dependent plasticity and normal cognitive function (Lewis et al., 2005), identifying these molecular mechanisms in inhibitory neurons is key to understanding how cortical circuits respond to sensory input.

Inhibitory neurons regulate cortical function by controlling action potential generation, preventing runaway excitation, sharpening excitatory neuron tuning, and entraining oscillatory firing of cohorts of excitatory neurons (Isaacson and Scanziani, 2011; Somogyi and Klausberger, 2005). Subtypes of inhibitory neurons differ from each other with respect to their developmental lineage, morphology, gene expression program, electrophysiological properties, and postsynaptic targets (Markram et al., 2004). Despite this diversity, inhibitory neurons can be broadly grouped into three nonoverlapping functionally distinct subtypes based on whether they express somatostatin (SST), parvalbumin (PV), or the 5HT3a receptor (Rudy et al., 2011). A variety of cellular mechanisms have been identified that mediate the response of inhibitory neurons to sensory input; for instance, sensory experience promotes the maturation of inhibitory neurons by increasing their membrane excitability during brain development and by promoting the growth of dendritic and axonal arbors (Chattopadhyaya et al., 2004; Chen et al., 2011; Okaty et al., 2009). Excitatory synaptic inputs to inhibitory neurons also undergo changes in response to activity, including short- and long-lasting plasticity (Kullmann et al., 2012). Despite this increased understanding of the cellular basis of inhibitory neuron plasticity, the molecular mechanisms by which neuronal activity affects the development and plasticity of excitatory synapses onto inhibitory neurons are poorly characterized.

Studies of excitatory neurons have revealed that neuronal activity regulates synapse development and function through several distinct mechanisms, including the transcriptional induction of regulators of synaptic function (Flavell and Greenberg, 2008). Upon membrane depolarization, calcium enters neurons through NMDA receptors and L-type calcium channels and initiates a signaling cascade that activates pre-existing transcription factors. These factors then induce the transcription of early-response genes, which are enriched for additional transcription factors (e.g., *Fos*, *Npas4*, *Zif268*) that subsequently promote the transcription of late-response genes. These late-induced

genes include regulators of synaptic connectivity that act locally at synaptic sites (e.g., *Bdnf*, *Cpg15/Nrn1*, *Homer1*). In excitatory neurons, this gene network functions to promote neuronal survival and dendritic morphogenesis, as well as to restrict the number of excitatory synapses and increase the number of inhibitory synapses that form on excitatory neurons (Bloodgood et al., 2013; Hong et al., 2008; Lin et al., 2008).

Npas4 is an early-response transcription factor that is enriched in the brain and induced in excitatory neurons specifically upon calcium influx and that has been suggested to regulate excitatory-inhibitory balance within neural circuits (Bloodgood et al., 2013; Coutellier et al., 2012). Npas4 deletion leads to an impairment of several forms of neuronal plasticity, suggesting that expression of Npas4 is necessary for the nervous system to adapt to sensory input (Maya-Vetencourt et al., 2012; Ploski et al., 2011; Ramamoorthi et al., 2011).

We show here that neuronal activity induces a distinct Npas4-dependent gene program in inhibitory neurons that functions to promote the development of excitatory synapses on SST-positive inhibitory neurons. Though neuronal activity induces the same early-response transcription factors such as Npas4 in both excitatory and inhibitory neurons, it induces distinct but overlapping sets of late-response genes in these two types of neurons. This allows the synapses that form on inhibitory and excitatory neurons to be modified by neuronal activity in a manner specific to their function within a circuit. In excitatory neurons, Npas4 activates transcription of *Bdnf*, thereby promoting an increased number of inhibitory synapses on excitatory neurons. In SST neurons, Npas4 regulates a distinct set of target genes that serve to increase excitatory input onto SST neurons, likely resulting in enhanced feedback inhibition within cortical circuits. Thus, the same activity-regulated transcription factor, by controlling distinct networks of genes, differentially regulates synaptic input to excitatory and inhibitory neurons, thereby facilitating appropriate circuit responses to sensory experience.

RESULTS

To study activity-dependent gene expression in inhibitory neurons, we prepared neuronal cultures highly enriched for these neurons by taking advantage of the fact that, early in their development, inhibitory neurons are localized to specialized regions of the embryonic brain, the ganglionic eminences, that are devoid of excitatory neurons (Wonders and Anderson, 2006). We dissected the medial ganglionic eminence (MGE) at embryonic day 14 (E14), dissociated the tissue, and maintained the resulting cells in vitro for 10 days (Figure 1A). We find by immunostaining, western blot, quantitative RT-PCR (qPCR), and microarray analysis (see below) that MGE cultures are highly enriched for the inhibitory markers Gad65/67 (Figures 1B–1D and S1A and S1G). Conversely, MGE cultures are almost completely devoid of markers of excitatory neurons such as Vglut1 (*Slc17a7*) and Tbr1 and of glia-specific GFAP (Figures 1D, S1A, S1C, and S1G). Moreover, by immunostaining with antibodies directed against markers of various inhibitory neuron subtypes, we find that MGE cultures contain a variety of inhibitory neuron subtypes that match the subtypes found in the MGE in vivo (Figure S1C; Markram et al., 2004). Finally, using double immunolabeling for pre- and postsynaptic marker proteins (Figure S1D) and electrophysiological recordings of miniature synaptic currents (data not shown), we detect a large number of inhibitory synapses but very few excitatory synapses in MGE cultures. For the purpose of comparison, we also prepared cultures that are devoid of inhibitory neurons by dissecting and dissociating the mouse cortex at E14, a time during brain development before most inhibitory neurons have migrated to the cortex (named from here on CTX cultures; Figure 1A). DIV10 CTX cultures are almost completely devoid of Gad65/67-positive neurons, and they contain substantially more Vglut1 (*Slc17a7*) mRNA than MGE cultures (Figures 1B–1D and S1G). Thus, MGE and CTX cultures are highly enriched for inhibitory and excitatory neurons, respectively, and as such should be useful for examining how neuronal activity affects gene expression in these two subsets of neurons.

Activity-Induced Gene Expression in Inhibitory Neurons

To identify the activity-dependent gene program in inhibitory neurons, MGE cultures were incubated with TTX and AP-5 to block sodium channels and NMDA receptors, respectively, and were then exposed to elevated levels of potassium chloride (55 mM KCl) to induce membrane depolarization and calcium influx. RNA was purified from samples after 0, 1, and 6 hr of stimulation, and microarray analysis was performed. We also performed a similar depolarization experiment using CTX cultures so that we could compare the activity-dependent gene program induced in those two neuronal subpopulations.

In MGE cultures, almost all of the probe sets maximally induced after 1 hr of membrane depolarization (26 out of 28) were also induced in CTX cultures 1 hr after depolarization, indicating that the early transcriptional response to membrane depolarization is very similar in MGE and CTX cultures (Figures 1E and 1F). As in excitatory neurons, the set of early-response genes in MGE cultures is significantly enriched for transcriptional regulators (Gene Ontology term "Transcription Regulator Activity"; $p = 2.7 \times 10^{-4}$). Strikingly, 11 of the 12 transcriptional regulators acutely induced by neuronal activity in MGE-derived cultures are also induced in excitatory neurons and include immediate-early genes such as *Fos*, *FosB*, *Egr1-3*, *Nr4a1*, and *Npas4* that are known to robustly respond to neuronal activity and to mediate important neuronal functions (Table S3; Flavell and Greenberg, 2008). Thus, despite the opposing functions of excitatory and inhibitory neurons within a neural circuit, neuronal activity induces a common early-response gene program in excitatory and inhibitory neurons that is enriched for transcriptional activators (Figures 1E, 1F, and S1B).

We next asked whether the shared early-response transcription factors induced in both excitatory and inhibitory neurons regulate the same set of late-response genes or whether they regulate cell-type-specific sets of late-response genes that might mediate the response of specific neuronal subtypes to sensory input. To this end, we identified probe sets maximally induced 6 hr after membrane depolarization in MGE and CTX cultures and found a large number of late-induced probe sets in both cultures (MGE, 438 probe sets; CTX, 808 probe sets).

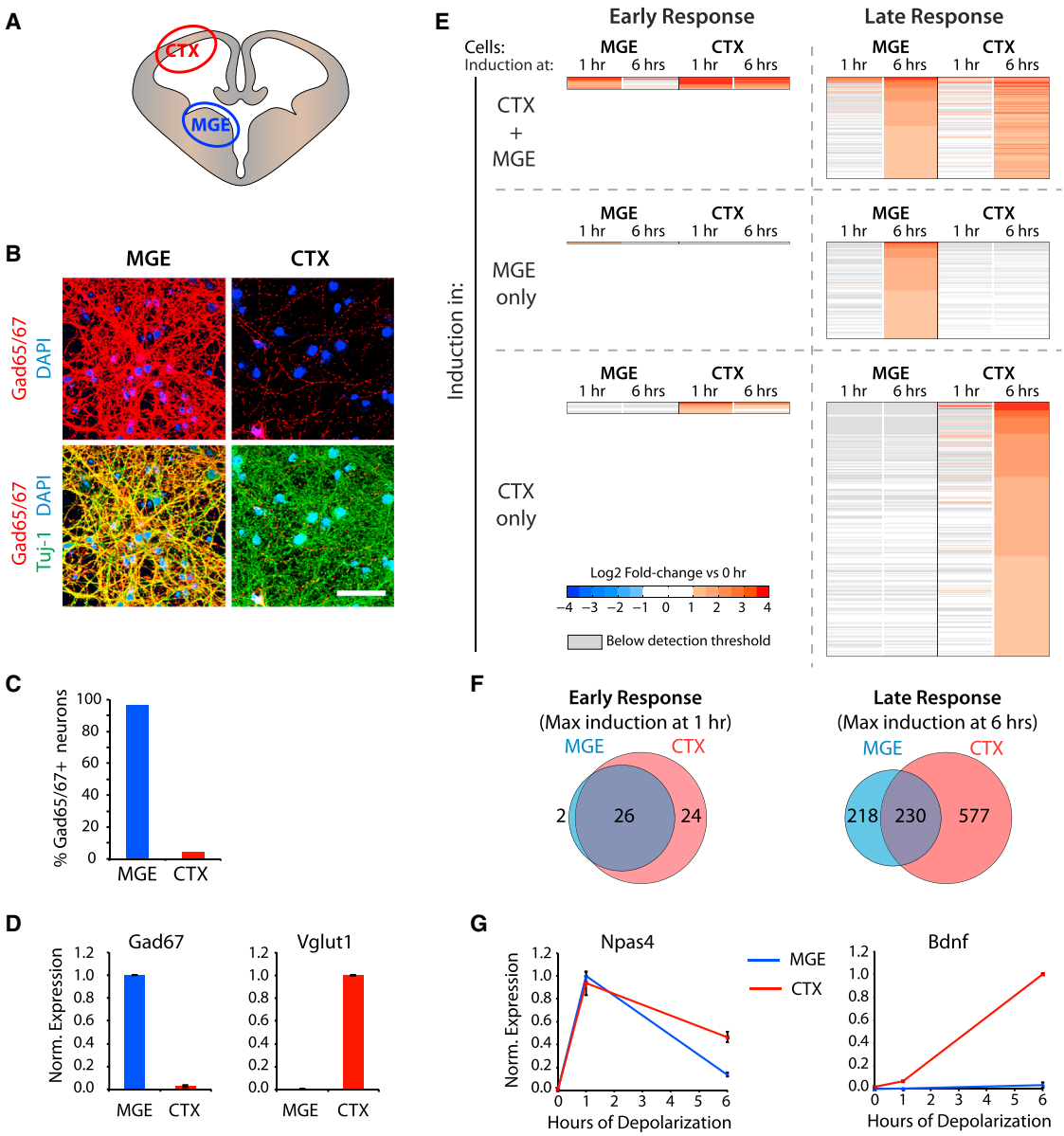

Figure 1. Activity-Induced Transcription in Inhibitory Neurons

(A–D) Separate dissection of the E14 medial ganglionic eminence and cortex yields cultures highly enriched for either inhibitory (MGE) or excitatory (CTX) neurons.

(A) Schematic coronal cross-section of the E14 mouse brain and the regions dissected to prepare MGE and CTX cultures.

(B) DIV10 MGE and CTX cultures immunostained for Gad65/67 (red, inhibitory neuron marker) and Tuj-1 (green, pan-neuronal marker) (DAPI, blue; scale bar, 50 μm).

(C) Quantification of Tuj-1-positive neurons that stain positive for Gad65/67 in MGE or CTX cultures.

(D) qPCR analysis for Gad67 (*Gad1*) and Vglut1 (*Slc17a7*) in DIV10 MGE (blue) and CTX (red) cultures. Data are represented as mean ± SEM of three bioreps.

(E–G) Genome-wide analysis of the gene program induced by neuronal activity in inhibitory and excitatory neurons: shared early-induced genes and cell-type-specific late-induced genes.

(E) Heatmaps showing results of the microarray analysis of membrane-depolarized MGE or CTX cultures. Displayed are all probe sets changing by 2-fold or more in at least one condition; each horizontal line represents the fold changes of one probe set.

(F) Venn diagrams displaying the number of probe sets induced after 1 or 6 hr of membrane depolarization specifically in MGE cultures (blue), specifically in CTX cultures (red), or commonly in both types of cultures (purple).

(G) qPCR analysis for *Npas4* and *Bdnf* in DIV10 MGE (blue) and CTX cultures (red) after 0, 1, or 6 hr of membrane depolarization. Data are represented as mean ± SEM of three bioreps.

See also Figure S1.

However, only ~25% of these probe sets (230 out of 1025) are induced in both MGE and CTX cultures, indicating that neuronal activity induces distinct sets of late-response genes in excitatory and inhibitory neurons (Figures 1E and 1F). These findings were corroborated by high-throughput sequencing of MGE cultures (RNA-seq) and qPCR experiments (Figures 1G and S1F). Stimulation of MGE and CTX cultures with glutamate confirmed that common sets of early-response genes and distinct sets of late-response genes are activated by multiple activity paradigms in vitro (Figure S1E). Taken together, these analyses indicate that inhibitory and excitatory neurons share a common set of rapidly induced transcription factors that likely regulate distinct sets of late-response genes.

To determine whether neuronal activity driven by sensory experience in vivo also induces shared early-response genes and distinct sets of late-response genes in inhibitory and excitatory neurons, we generated mice heterozygous for alleles of either Emx1-Cre (expressed specifically in excitatory neurons) or Gad2-Cre (expressed specifically in inhibitory neurons) harboring the *Rpl22-HA* (*RiboTag*) allele, which expresses an HA-tagged ribosomal subunit specifically in Cre-expressing neurons (Sanz et al., 2009). The resulting animals permit the immunopurification of ribosomally associated RNAs selectively from either excitatory or inhibitory neurons using anti-HA antibodies. qPCR analysis of cell-type-specific marker genes showed that samples immunopurified from Emx1-Cre mice were highly enriched for *Tbr1* and Vglut1 (*Slc17a7*) mRNA, whereas samples from Gad2-Cre mice were highly enriched for Gad65 (*Gad2*) and Gad67 (*Gad1*) mRNA (Figure 2A).

With this approach, we examined the cell-type-specific regulation of selected activity-responsive genes in vivo. RiboTag animals maintained in the dark were exposed to light for 0, 1, 3, or 7.5 hr, their visual cortices dissected, and ribosomal-associated RNA immunopurified from either excitatory or inhibitory neurons. qPCR analysis of the resulting immunoprecipitates confirms the induction of a common set of early-response factors, including *Egr1*, *Fos*, *FosB*, and *Npas4* in both inhibitory and excitatory neurons (Figure 2B). Although a subset of late-response genes shared between excitatory and inhibitory cell types is apparent (e.g., *Fosl2*, *Gpr3*, *Rgs2*, and *Vgf*), we also observe cell-type-specific regulation of late-response genes that recapitulated the expression patterns observed in vitro, including late-response genes specific to either inhibitory (e.g., *E530001K10RIK*, *Igf1*, *Pnoc*, *Pthlh*) or excitatory (e.g., *Adcyap1*, *Bdnf*, *Nrn1*, and *Ptgs2*) neurons (Figures 2C–2E). Taken together, these experiments demonstrate that sensory experience induces shared sets of early-response genes and distinct but overlapping sets of late-response genes in excitatory and inhibitory neurons in vivo in an intact neural circuit. Furthermore, these in vivo experiments confirm that MGE and CTX cultures are a useful paradigm for studying the cell-type-specific molecular events that occur in response to neuronal activity in inhibitory and excitatory neurons.

Npas4 Is Induced by Neuronal Activity across Inhibitory Neuron Subtypes

Rather than focus on a single late-response gene induced selectively in MGE cultures, to assess the general function of the activity-dependent gene program in inhibitory neurons, we investigated the function of a shared early-response transcription factor, Npas4. Because Npas4 promotes inhibitory synapse development on excitatory neurons by activating *Bdnf* but *Bdnf* is not expressed in inhibitory neurons in vitro or in vivo, we hypothesized that Npas4 induces distinct sets of late-response genes in excitatory or inhibitory neurons, thereby mediating cell-type-specific responses that are tuned to the function of a neuron within a circuit. By identifying the specific function of Npas4 and its transcriptional targets in inhibitory neurons, we might characterize the molecular response of inhibitory neurons to activity.

We first asked which inhibitory neuron subtypes express Npas4 in vitro in response to membrane depolarization and in vivo in response to sensory stimulation. We membrane depolarized E16.5 mixed cortical cultures and immunostained for Npas4 and marker proteins that are selectively expressed in distinct inhibitory neuron subtypes. Upon membrane depolarization, each of the inhibitory neuron subtypes examined expresses Npas4 (Figures S2A and S2B). To assess Npas4 expression in vivo, we generated mice in which genetically defined subtypes of inhibitory neurons were fluorescently labeled. These mice were dark housed for several days and perfused either without having been exposed to light (dark housed) or after 2.5 hr of light exposure (light exposed). We immunolabeled brain sections with anti-Npas4 antibodies and quantified the percentage of each inhibitory neuron subtype that stained positive for Npas4. No Npas4-positive inhibitory neurons were observed in the visual cortex of dark-housed mice; however, upon light exposure, we find induction of Npas4 expression in all inhibitory neuron types analyzed (e.g., Dlx5/6, PV, SST, VIP) (Figure 2F). Consistent with our in vitro results, Npas4 is expressed in SST- and VIP-positive neurons and in a smaller fraction of PV-positive neurons (Figure 2G). This pattern of Npas4 induction is also observed when subtypes of inhibitory neurons were identified using antibodies that recognize proteins that are selectively expressed in specific inhibitory neuron subtypes (Figure S2C). Taken together, these data demonstrate that Npas4 is induced in multiple inhibitory neuron subtypes in vitro upon membrane depolarization and in vivo after sensory stimulation.

Npas4 Regulates the Development of Excitatory Synapses onto SST Neurons

To investigate the function of Npas4 in inhibitory neurons, we focused on SST-expressing neurons because Npas4 is highly induced in these neurons and because SST neurons mediate feedback inhibition to pyramidal neuron dendrites (Silberberg and Markram, 2007). Because SST neurons receive local excitatory input and form dense networks of inhibitory synapses onto nearby pyramidal neurons (Fino and Yuste, 2011), we hypothesized that they are optimally situated within a cortical circuit to utilize activity-induced transcriptional pathways to read out local levels of activity and mount a homeostatic response. To test this idea, we selectively removed Npas4 from SST neurons and prepared dissociated E16.5 mixed cortical cultures from embryos heterozygous for an allele expressing Cre recombinase under the control of the endogenous *Somatostatin* locus (SST-Cre) and an allele harboring a Cre-dependent tdTomato fluorescent

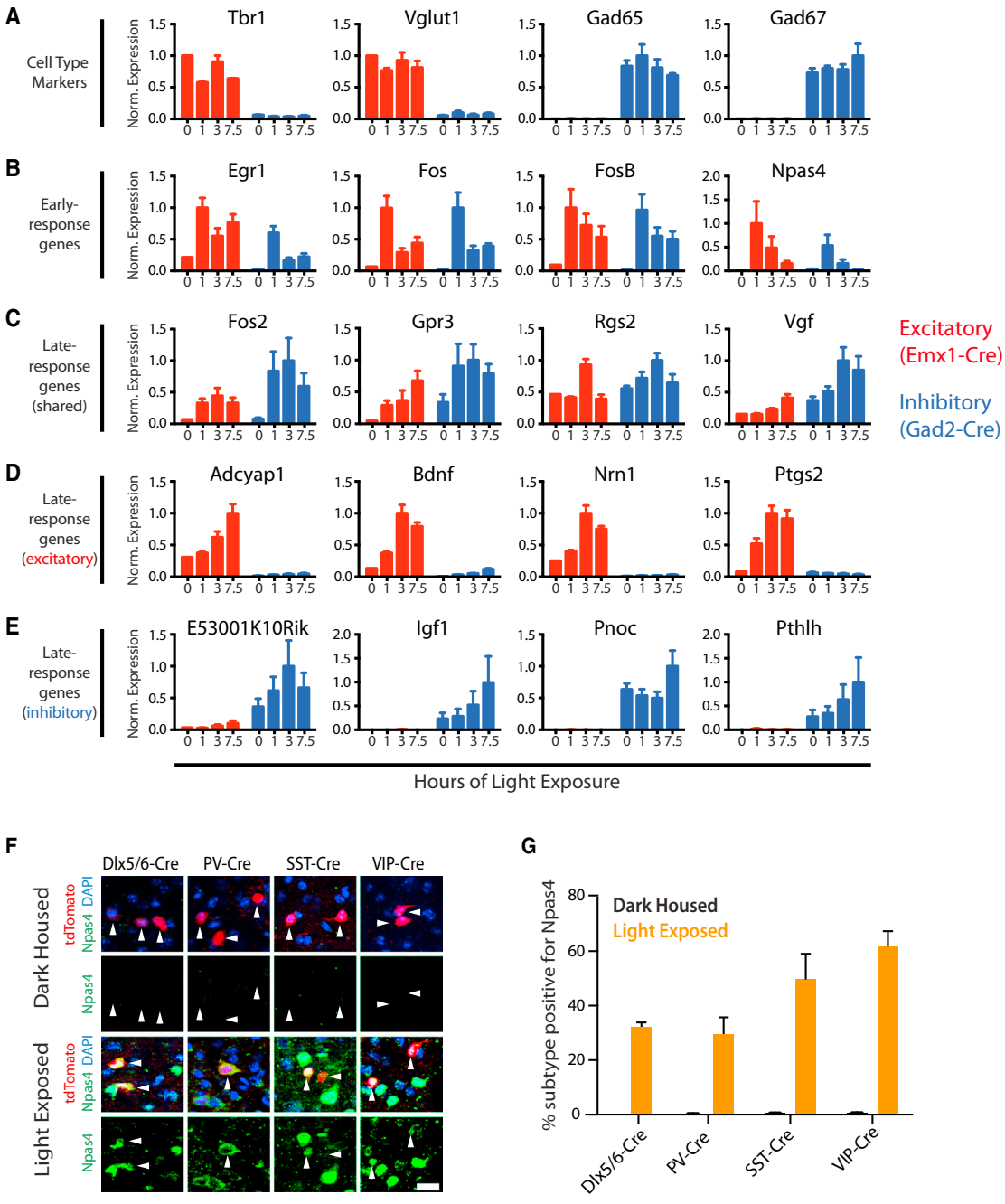

Figure 2. Experience-Dependent Gene Induction in Inhibitory Neurons In Vivo

(A–E) Sensory experience induces shared sets of early-response transcription factors and distinct sets of late-response effector genes in inhibitory and excitatory neurons in vivo. Normalized expression of ribosome-associated RNA purified from the visual cortex of Emx1-Cre-expressing (red) or Gad2-Cre-expressing (blue) neurons in dark-housed mice (0 hr) and after light exposure (1, 3, 7.5 hr). Data are represented as mean + SEM of three bioreps.

(A) Cell-type-specific marker genes.

(B) Early-response genes predicted by in vitro experiments to be induced in both excitatory and inhibitory neurons.

(C–E) Late-response genes predicted by in vitro experiments to be induced in (C) both excitatory and inhibitory neurons, (D) only in excitatory neurons, and (E) only in inhibitory neurons.

(F and G) Npas4 is induced by sensory experience in multiple inhibitory neuron subtypes.

(F) Immunostaining of visual cortices of mice dark housed and light exposed for 2.5 hr. Inhibitory neuron subtypes are labeled by Cre-dependent expression of tdTomato (red, driven by Dlx5/6-Cre, PV-Cre, SST-Cre, or VIP-Cre) and with antibodies against Npas4 (green) (coronal sections; scale bar, 5 μm).

(G) Quantification of (F). Data are represented as mean + SEM of three bioreps.

See also Figure S2.

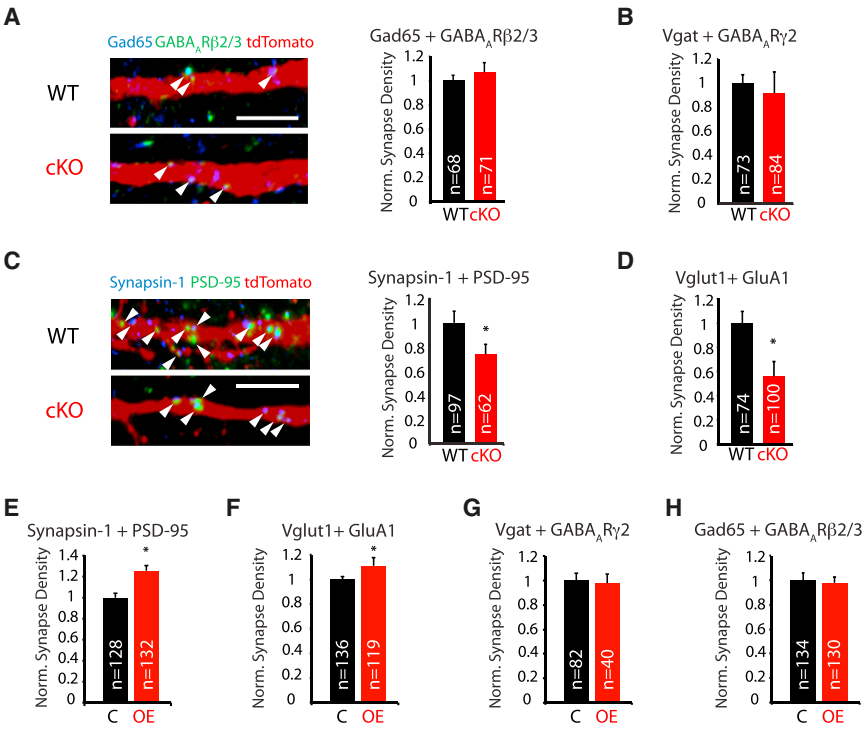

Figure 3. Npas4 Regulates Excitatory, but Not Inhibitory, Synapse Number in SST Neurons

Synapse assays in E16.5 mixed cortical cultures immunostained for pairs of pre- and postsynaptic markers. Synapse density was determined by quantifying colocalized puncta of pre- and postsynaptic markers that overlap with either tdTomato-positive (A–D) or GFP-positive (E–H) SST neuron dendrites (A and C: arrowheads indicate synapses; scale bars, 5 μm). Data were normalized to the mean synapse density in each control condition; data represent the mean + SEM of three bioreps; $^*p < 0.05$.

(A–D) cKO of Npas4 in SST neurons reduces the number of excitatory, but not inhibitory, synapses formed onto Npas4 cKO SST neurons. Cultures were prepared from littermate Npas4 WT or cKO embryos that are heterozygous for alleles of SST-Cre and Cre-inducible tdTomato. (A) Inhibitory synapse markers GABA$_A$R β2/3 (green) + Gad65 (blue) and (B) Vgat and GABA$_A$Rγ2, (C) excitatory synapse markers PSD-95 (green) + Synapsin-1 (blue), and (D) Vglut1 + GluA1.

(E–H) Overexpression of Npas4 in SST neurons increases the number of excitatory, but not inhibitory, synapses formed onto SST neurons. Cultures were prepared from SST-Cre embryos, infected at DIV4 with lentiviral constructs driving in a Cre-dependent manner the expression of Npas4 and GFP (OE) or only GFP (C) and maintained until DIV8. (E) Excitatory synapse markers PSD-95 + Synapsin-1 and (F) Vglut1 + GluA1 and (G) inhibitory synapse markers Vgat + GABA$_A$Rγ2 and (H) GABA$_A$Rβ2/3 + Gad65.

See also Figure S3.

reporter. These embryos were homozygous for either a wild-type allele of Npas4 (WT) or an Npas4 allele flanked by LoxP sites, allowing for Cre-dependent Npas4 deletion (cKO) (Lin et al., 2008). SST-Cre functions effectively in SST-expressing neurons, as most tdTomato-positive neurons were also positive for staining with anti-Somatostatin antibodies (Figure S3A). Furthermore, SST-Cre efficiently excised the floxed Npas4 allele, as KCl-induced Npas4 expression in tdTomato-labeled SST neurons is abolished in cKO cultures (Figure S3B).

To assess whether Npas4 regulates the development of inhibitory synapses formed onto SST-positive neurons, as it does in excitatory neurons, we quantified the density of inhibitory synapses formed onto SST neurons by immunolabeling WT and cKO cultures with antibodies directed against two sets of markers for inhibitory synapses, Gad65/GABA$_A$Rβ2/3 and Vgat/GABA$_A$Rγ2. We then counted the number of pre- and postsynaptic marker co-clusters that overlapped with fluorescently labeled SST neuron dendrites and divided by the total dendritic area. This analysis revealed that, in contrast to the effect of Npas4 deletion in excitatory neurons, deletion of Npas4 has no effect on the density of inhibitory synapses formed onto SST-expressing neurons (Figures 3A and 3B).

To determine the effect of Npas4 loss on the development of excitatory inputs onto SST neurons, we quantified the density of excitatory synapses formed onto SST neurons. We find that selective deletion of Npas4 in SST neurons results in a significantly lower density of excitatory synapses on SST neurons as measured by the overlap of two independent sets of excitatory synapse markers, Synapsin-1/PSD-95 and Vglut1/GluA1 (Figures 3C and 3D). Importantly, the effect of Npas4 deletion on excitatory synaptic connections onto SST neurons is not due to an indirect effect of Npas4 deletion on neuronal survival, cell size, or the complexity of proximal dendrites (Figures S3C and S3D and data not shown).

We next determined whether overexpression of Npas4 in SST neurons is sufficient to drive an increase in excitatory synapse density. We infected E16.5 mixed cortical cultures from SST-Cre embryos with lentiviral constructs that in a Cre-dependent manner express either Npas4 together with GFP or GFP alone. After confirming that expression of Npas4 and/or GFP in these cultures is restricted to SST neurons (Figure S3E), we quantified the density of synapses as before. Overexpression of Npas4 in SST neurons causes an increase in the density of excitatory synapses but has no effect on the number of inhibitory synapses that form on SST neurons (Figures 3E–3H). These findings indicate that Npas4 controls the number of excitatory, but not inhibitory, synaptic inputs onto SST neurons. This function is different from Npas4's previously described function in excitatory neurons (Bloodgood et al., 2013; Lin et al., 2008) and suggests that Npas4 functions in a cell-type-specific manner to control excitatory-inhibitory balance.

To determine whether these morphological changes reflect alterations in functional excitation, we used the genetic strategy described above to conditionally delete Npas4 from SST

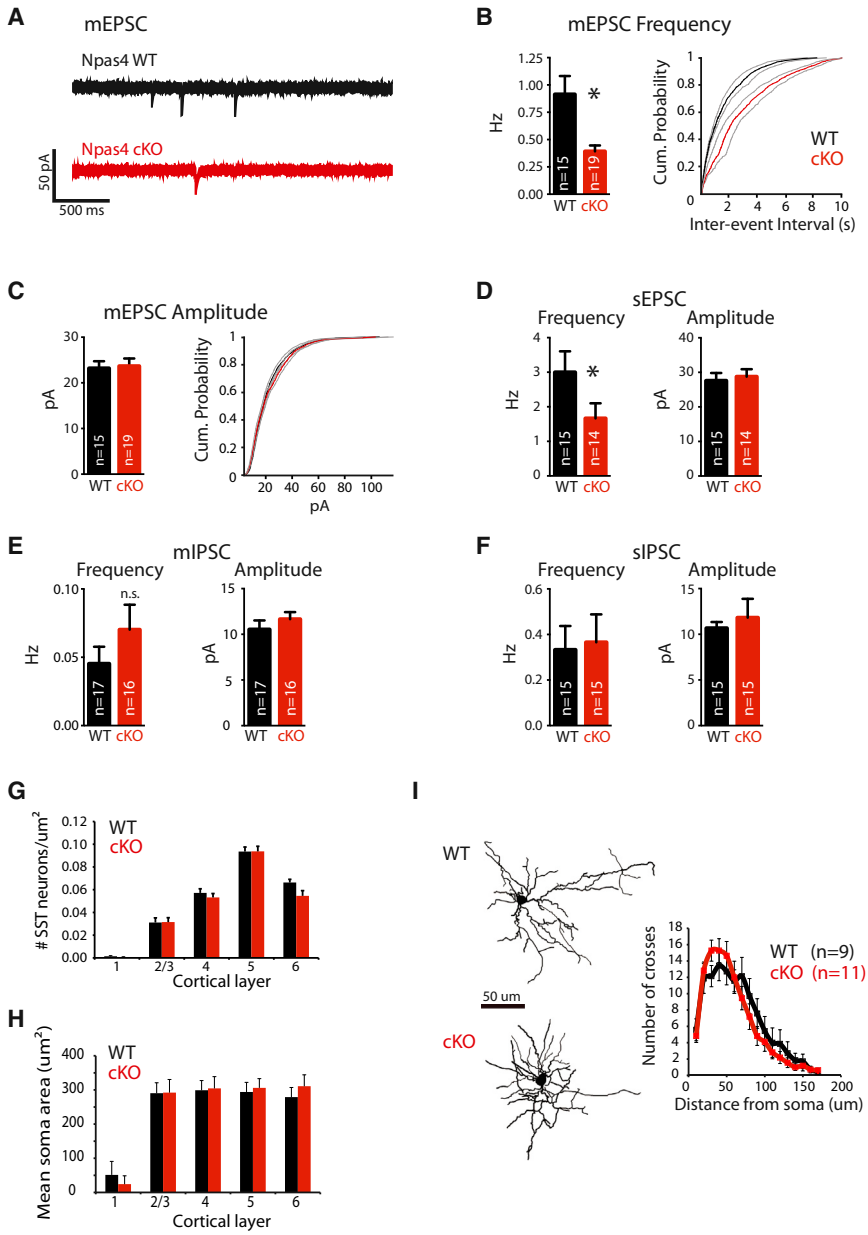

Figure 4. Npas4 Regulates the Development of Functional Excitatory Inputs onto SST Neurons

(A–F) Deletion of Npas4 in SST neurons reduces functional excitation, but not inhibition, onto SST neurons in the visual cortex in vivo. Whole-cell patch-clamp recordings were obtained from tdTomato-labeled SST neurons in acute slices of Npas4 WT (black) or cKO (red) P10–P12 mice. Data presented as bar graph of mean + SEM or as cumulative distribution function CDF of mean ± SEM; *p < 0.05.

(A) Example traces of miniature EPSCs (mEPSCs) (recorded at −70 mV in the presence of 0.5 μM TTX, 50 μM picrotoxin, and 25 μM cyclothiazide; scale bar, 50 pA, 500 ms).

(B) (Left) mEPSC frequency (p < 0.005, Mann-Whitney U test). (Right) CDF of the mEPSC inter-event intervals of all neurons sampled in each genotype.

(C) (Left) mEPSC amplitude (p = 0.847, Mann-Whitney U test). (Right) CDF of the mEPSC event amplitudes of all neurons sampled in each genotype.

(D) (Left) Spontaneous EPSC (sEPSC) frequency (recorded at −70 mV in the presence of 50 μM PTX; p = 0.027, Mann-Whitney U test). Right, sEPSC amplitude (p = 0.499, Mann-Whitney U test).

(E) (Left) mIPSC frequency (recorded at 0 mV in the presence of 0.5 μM TTX, 25 μM NBQX, and 50 μM CPP; p = 0.261, Mann-Whitney U test). (Right) mIPSC amplitude (p = 0.386, Mann-Whitney U test).

(F) (Left) sIPSC frequency (recorded at 0 mV in the presence of 25 μM NBQX and 50 μM CPP; p = 0.734, Mann-Whitney U test). (Right) sIPSC amplitude (p = 0.409, Mann-Whitney U test).

(G–I) Deletion of Npas4 in SST neurons does not affect the layer distribution, soma size, or dendritic complexity of SST neurons in the visual cortex. Density (G) and soma size (H) of tdTomato-labeled Npas4 WT (black) or cKO (red) SST neurons by cortical layer in P10–P12 visual cortices. Data are represented as mean + SEM of three bioreps. (I) Sholl analysis of dye-filled and reconstructed Npas4 WT (black) or cKO (red) SST neuron dendrites in the P11 visual cortex. (Left) Example images (scale bar, 50 μm). (Right) quantification (p = 0.244, repeated-measures ANOVA).

See also Figure S4.

neurons and obtained whole-cell patch-clamp recordings from these cells in acute slices from postnatal days 10–12 (P10–P12) WT or cKO animals (Figures 4A–4F), an age range that closely matches the developmental stage of the neurons analyzed in culture. At P10–P12, calcium waves sweep through the cortex before eye opening, providing a source of neuronal activity to activate Npas4 (Garaschuk et al., 2000), and widespread Npas4 expression is observed in SST neurons at P11 following kainate seizure induction (Figure S2D). Importantly, at this age, SST-Cre efficiently excises the Npas4-floxed allele in vivo and promotes expression of tdTomato in SST, but not VIP- or PV-positive neurons (Figures S4B and S4C).

Conditional deletion of Npas4 results in a significant decrease in the frequency of pharmacologically isolated miniature excitatory postsynaptic currents (mEPSCs) (WT: 0.91 ± 0.168 Hz, n = 15; cKO: 0.39 ± 0.054 Hz, n = 19; p = 0.003; Figures 4A and 4B), which are blocked by NBQX and CPP treatment (Figure S4D; n = 3). We observe no change in mEPSC amplitude or kinetics (WT: 23.19 ± 1.54 pA, n = 15; cKO 23.64 ± 1.68 pA, n = 19; p = 0.847; Figures 4C and S4E), suggesting that deletion of Npas4 from SST neurons selectively alters mEPSC frequency. This decrease in mEPSC frequency could be due to decreased presynaptic probability of release or could result from a decrease in the number of functional excitatory synapses onto SST

neurons. Given that this effect is observed following the selective deletion of Npas4 from SST neurons, together with the observed reduction in the density of excitatory synaptic connections formed onto SST neurons in vitro when Npas4 is deleted, our data are consistent with a change in the number of functional excitatory synapses onto SST neurons in vivo when Npas4 is deleted from SST neurons.

To investigate the effect of selective Npas4 deletion on the functional excitatory drive impinging upon SST neurons, we recorded EPSCs in the absence of bath-applied TTX (e.g., spontaneous EPSCS [sEPSCs]) from SST neurons in acute visual cortex slices of P10–P12 WT or cKO mice. Loss of Npas4 results in a significant decrease in the frequency of spontaneous EPSCs (WT: 2.99 ± 0.608 Hz, n = 15; cKO: 1.66 ± 0.437 Hz, n = 14; p = 0.027) but does not affect the amplitude of these events (WT: 27.57 ± 2.24 pA, n = 15; cKO: 28 ± 2.169 pA, n = 14; p = 0.499; Figure 4D), indicating that SST neurons lacking Npas4 receive reduced excitatory drive, which likely results in reduced firing.

Consistent with our observations in cultured neurons, no significant effect on mIPSC frequency (WT: 0.045 ± 0.012 Hz, n = 17; cKO: 0.07 ± 0.018 Hz, n = 16, p = 0.261) or amplitude (WT: 10.53 ± 0.98 pA, n = 17; cKO: 11.65 ± 0.772 pA, n = 16; p = 0.386) is observed in SST neurons in slice upon deletion of Npas4 (Figure 4E). Furthermore, spontaneous IPSCs in SST neurons are not affected by loss of Npas4 (Frequency WT: 0.33 ± 0.1 Hz, n = 15; cKO: 0.365 ± 0.122 Hz, n = 15; p = 0.7349; Amplitude WT: 10.66 ± 0.674 pA, n = 15; cKO: 11.81 ± 2.06 pA, n = 15; p = 0.4989; Figure 4F). Together, these data show that Npas4 regulates the amount of functional excitation, but not inhibition, on SST-positive inhibitory neurons in acute cortical slices.

To determine whether the effect of Npas4 on excitation onto SST neurons in vivo arises from a direct effect at the synapse or is a secondary effect on cell health, we compared visual cortex development of P10–P12 WT and cKO mice. The cortices of cKO mice are grossly normal as compared to their WT littermates (Figure S4A), and we find no change in the number or laminar distribution of SST neurons across the different cortical layers, indicating that Npas4 is not required for SST neuron migration, terminal differentiation, or survival (Figure 4G). Conditional deletion of Npas4 in SST neurons does not affect soma size (Figure 4H), and SST neurons lacking Npas4 extend and elaborate axons to target distal dendrites normally, as indicated by the presence of bright bands of tdTomato in layer 1 of the cortex of both genotypes (Figure S4A). In addition, Sholl analysis reveals that Npas4 does not regulate the dendritic complexity of SST neurons (WT: n = 9; cKO: n = 11; p = 0.244 repeated-measures ANOVA; Figure 4I). Taken together, this analysis demonstrates that removal of Npas4 from SST neurons affects neither overall cortical structure nor the number or morphology of SST neurons in the cortex.

In summary, our data indicate that, in contrast to Npas4's ability to stimulate an increase in the number of inhibitory synapses onto excitatory neurons, this activity-dependent transcription factor promotes the development of excitation on SST-positive inhibitory neurons. Given that inhibitory neurons do not express *Bdnf*, a major Npas4 target gene in excitatory neurons, it seemed likely that Npas4 regulates SST neuron connectivity by activating the transcription of a distinct set of late-response genes in inhibitory neurons.

Npas4 Regulates Cell Type-Specific Activity-Dependent Transcriptional Programs

We next identified the genes that Npas4 regulates in inhibitory neurons and compared them to those regulated by Npas4 in excitatory neurons. MGE cultures from littermate Npas4 WT or KO embryos were membrane depolarized for 0, 1, or 6 hr (Figure S5A), and mRNA from these cultures was analyzed by microarray and subsequent qPCR validation (Figure S5B). Deletion of Npas4 in MGE neurons has no effect on the early transcriptional response to membrane depolarization, but the induction of a set of late-response genes is compromised in the absence of Npas4 (Figures 5A, 5B, and 5G). To determine whether Npas4 specifically regulates these genes in inhibitory neurons as compared to excitatory neurons, we depolarized CTX cultures prepared from littermate Npas4 WT or KO embryos and performed microarray analysis. As in MGE cultures, loss of Npas4 has no effect on the induction of early-response genes in CTX cultures but does result in decreased induction of a specific subset of late-response genes (Figures 5C, 5D, and 5H). Comparative analysis revealed that Npas4-regulated genes in inhibitory neurons fall into two classes: some (e.g., *Rerg*, *Frmpd3*; Figure 5E) are induced by membrane depolarization only in MGE cultures, whereas others (e.g., *Nptx2*, *Gpr3*) are activity induced in both MGE and CTX cultures (Figure 5F). In total, half of the genes induced by membrane depolarization in an Npas4-dependent manner in MGE cultures were regulated by Npas4 in a cell-type-specific manner (9 genes Npas4 regulated only in MGE, 9 in MGE + CTX) (Figures 5E–5J). Additionally, 34 genes were regulated by Npas4 specifically in excitatory neurons (e.g., *Bdnf*, *Csrnp1*; Figure S5C). We conclude that Npas4 controls the expression of distinct but overlapping sets of activity-induced genes in inhibitory and excitatory neurons.

We next asked whether Npas4 overexpression is sufficient to induce the genes identified in the loss-of-function analysis in the absence of membrane depolarization and, if so, whether Npas4 functions in a cell-type-specific manner. We overexpressed Npas4 or GFP by lentiviral infections in MGE and CTX neurons, silenced the cells with TTX and AP-5, and then assessed the expression of genes found to be misregulated in the absence of Npas4. qPCR analysis showed that infection with the Npas4-expressing construct leads to a large increase in Npas4 expression and to significantly increased levels of the shared Npas4 targets *Gpr3* and *Nptx2* in both MGE and CTX cultures (Figure 5K). Strikingly, Npas4 overexpression results in significantly increased levels of the excitatory-specific Npas4 targets *Bdnf* and *Csrnp1* only in CTX cultures, whereas the levels of the MGE-specific Npas4 targets *Frmpd3* and *Rerg* increase significantly upon Npas4 overexpression only in MGE cultures (Figure 5K). These findings indicate that overexpressed Npas4 is sufficient to induce target gene expression in a cell-type-specific manner in the absence of other activity-regulated factors.

Npas4 regulates gene transcription by binding to the activity-dependent enhancers and promoters of its target genes (Kim

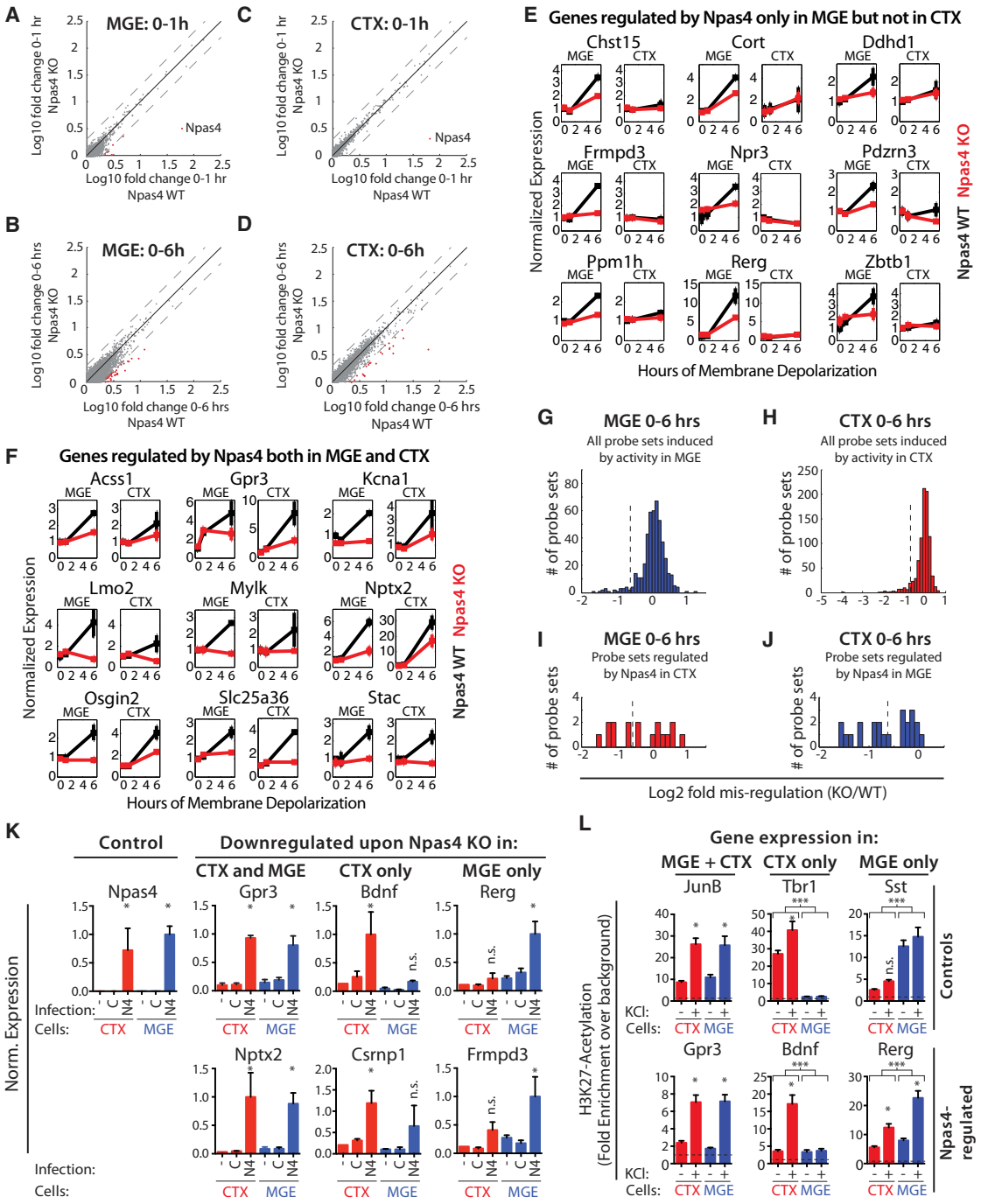

Figure 5. Npas4 Regulates a Cell-Type-Specific Activity-Induced Transcriptional Program in Inhibitory Neurons

(A-D) Microarray analysis of the depolarization-induced gene expression response in Npas4 WT or KO MGE and CTX cultures. Scatter plots show the fold change of every expressed probe set in WT cultures against its fold change in KO cultures. Black line, unity; dotted lines, 2-fold changes in either direction. Probe sets misregulated by more than 2-fold in the KO are labeled in red (the single strongly misregulated probe set in (A) and (C) represents Npas4). (A) Early response (0–1 hr) in MGE cultures. (B) Late response (0–6 hr) in MGE cultures. (C) Early response (0–1 hr) in CTX cultures. (D) Late response (0–6 hr) in CTX cultures.

(E–J) Analysis of microarray experiments. Npas4 controls the activity-dependent induction of distinct sets of late-response genes in inhibitory and excitatory neurons.

(E and F) Microarray-based line plots of genes regulated by Npas4 specifically in MGE neurons (E) or in both MGE and CTX neurons (F). Normalized expression is plotted versus duration of stimulus, and data are normalized to WT MGE 0 hr and presented as mean ± SEM of two bioreps (WT, black; KO, red).

(G and H) Histograms of all probe sets induced in MGE (G) and CTX (H) cultures showing the misregulation in Npas4 KO cultures. Probe sets to the left of the dotted lines are considered as Npas4 regulated.

(legend continued on next page)

et al., 2010). We hypothesized that Npas4 might achieve cell-type-specific activation of its target genes by binding to gene regulatory regions that function in a cell-type-specific manner in inhibitory and/or excitatory neurons. To test this idea, we identified *cis*-regulatory elements within 50 kb of Npas4 target genes that are inducibly bound by Npas4 upon membrane depolarization and exhibit histone modifications indicative of enhancer or promoter regions. ChIP-seq data sets (Kim et al., 2010) generated from mixed cortical cultures containing both excitatory and inhibitory neurons using anti-Npas4, -CBP, -H3K4me1, and -H3K4me3 antibodies revealed that most Npas4-regulated genes are located near candidate regulatory elements (6 out of 9 genes regulated by Npas4 in MGE only, 9/9 regulated in MGE + CTX, 31/34 regulated in CTX only; Figure S5D).

To test whether these elements are activated in a cell-type-specific manner upon membrane depolarization, we conducted chromatin immunoprecipitation (ChIP) experiments on nuclear extracts from MGE and CTX cultures with antibodies to acetylated lysine 27 of histone H3 (H3K27Ac), a histone mark that demarcates transcriptionally active regulatory elements (Creyghton et al., 2010). H3K27Ac enrichment at the regulatory regions of *Tbr1* (expressed only in CTX) and *Sst* (MGE-specific) accurately tracks with the respective expression of these loci in MGE and CTX cultures (Figure 5L). H3K27Ac levels also increase significantly at the Npas4-bound gene regulatory regions of JunB (an early-response gene induced in both cell types) and Gpr3 (an Npas4 target in both cell types) in both culture types after membrane depolarization. In contrast, membrane depolarization led to increased H3K27Ac levels at a regulatory element associated with Bdnf (regulated by Npas4 specifically in excitatory neurons) only in CTX cultures, whereas H3K27Ac levels at the regulatory region of Rerg (regulated by Npas4 only in inhibitory neurons) increase following membrane depolarization selectively in MGE cultures. These data suggest that the transcriptional outcome of Npas4 induction in excitatory and inhibitory neurons is defined at least in part by the cell-type-specific status of the regulatory elements of Npas4 target genes.

Npas4 Regulates an Experience-Induced Gene Program in SST Neurons

Finally, we sought to identify Npas4-regulated genes in SST neurons that might mediate the Npas4-dependent effects on neuronal connectivity in these cells. We employed the RiboTag-approach to immunopurify RNA from the visual cortex of dark-housed and light-exposed mice that express the RiboTag allele in either SST neurons (labeled by SST-Cre) or excitatory neurons (labeled by Emx1-Cre). qPCR analysis for a set of cell-type-specific control genes indicated that the RNA immunopurified from SST-Cre-expressing neurons is highly enriched for *Sst* and Gad67 (*Gad1*) mRNA, whereas RNA immunopurified from Emx1-Cre-expressing neurons is enriched for Vglut1 (*Slc17a7*) mRNA (Figure 6A). As expected, light exposure results in a robust increase in the levels of the ribosome-associated mRNAs of the early-response genes *Npas4* and *Fos* in both Emx1- and SST-Cre-expressing neurons (Figure 6B). We then examined 14 of the Npas4-regulated genes identified in MGE cultures. mRNA corresponding to four of these loci (*Frmpd3*, *Slc25a36*, *Kcna1*, *Ddhd1*) is significantly induced following light exposure in SST neurons, but not in excitatory neurons, and the levels of six more Npas4-regulated genes (*Stac*, *Osgin2*, *Nptx2*, *Ppm1h*, *Bach2*, *Gpr3*) are increased upon light stimulation in both excitatory and SST neurons (Figures 6C and 6D; Induction: 1, 3, 7.5 hr > 30% change from max 0 hr value). Levels of the four remaining genes do not increase in response to light exposure in SST neurons, suggesting that elements of the Npas4-regulated gene program in MGE cultures may be specific to other inhibitory neuron subtypes (Figure 6E).

To identify which of these activity-responsive genes are dependent on Npas4 in vivo, we compared light-dependent induction of these genes in the visual cortex of dark-housed wild-type and Npas4 KO mice (Figure 6F). qPCR analysis demonstrates that all four of the Npas4 targets induced by light exposure specifically in SST neurons show reduced upregulation in Npas4 KO mice. In addition, three of the six Npas4-regulated genes that are induced upon light exposure in both SST and excitatory neurons are misregulated in Npas4 KO mice (*Gpr3*, *Nptx2*, *Osgin2*). To begin to test whether Npas4 regulates the expression of these genes specifically in SST neurons in vivo, we immunolabeled brain sections of mice that lack Npas4 in SST neurons with antibodies that recognize Narp, the protein product of the Npas4 target *Nptx2*. Quantitative immunofluorescence analysis confirmed that the level of Narp is reduced in SST neurons when Npas4 is deleted in these neurons (Figures 6G and 6H). In summary, these results demonstrate that a distinct Npas4-driven gene program is induced in SST neurons in response to sensory experience. Intriguingly, several of these Npas4 target genes in SST neurons have been reported to act

(I) Histogram showing the misregulation in Npas4 KO MGE cultures of all genes regulated by Npas4 in CTX cultures. Probe sets to the right of the dotted line are considered as Npas4 regulated specifically in CTX neurons.

(J) Histogram showing the misregulation in Npas4 KO CTX cultures of all genes regulated by Npas4 in MGE cultures. Probe sets to the right of the dotted line are considered as Npas4 regulated specifically in MGE neurons.

(K) Npas4 overexpression (OE) induces cell-type-specific Npas4 target gene expression in the absence of neuronal activity. qPCR analysis of expression levels of cell-type-specific and shared Npas4 targets after Npas4-OE in CTX (red) or MGE (blue). The cultures were either not infected (–) or infected at DIV4 with constructs expressing GFP (C) or Npas4 (N4), quieted O.N. at DIV7, and harvested on DIV8. Data represent the mean + SEM of four bioreps; *, significantly changed; $p < 0.05$, one-way ANOVA with Sidak's multiple comparison correction.

(L) Cell-type-specific activation status of gene regulatory elements associated with Npas4 target genes reflects the cell-type-specific regulation by Npas4. H3K27Ac ChIP on DNA isolated from CTX (red) and MGE cultures (blue) ± KCl depolarization. qPCR was done either on regulatory regions associated with control genes or on Npas4-binding regulatory regions associated with genes regulated by Npas4. Data are presented as mean + SEM of fold enrichment above background (dashed black line; n = 4 bioreps for CTX, n = 5 bioreps for MGE; *, significant change of H3K27Ac levels within a cell type; ***, significant difference of H3K27Ac across CTX and MGE; *p and ***$p < 0.05$, one-way ANOVA with Sidak's multiple comparison correction).

See also Figure S5.

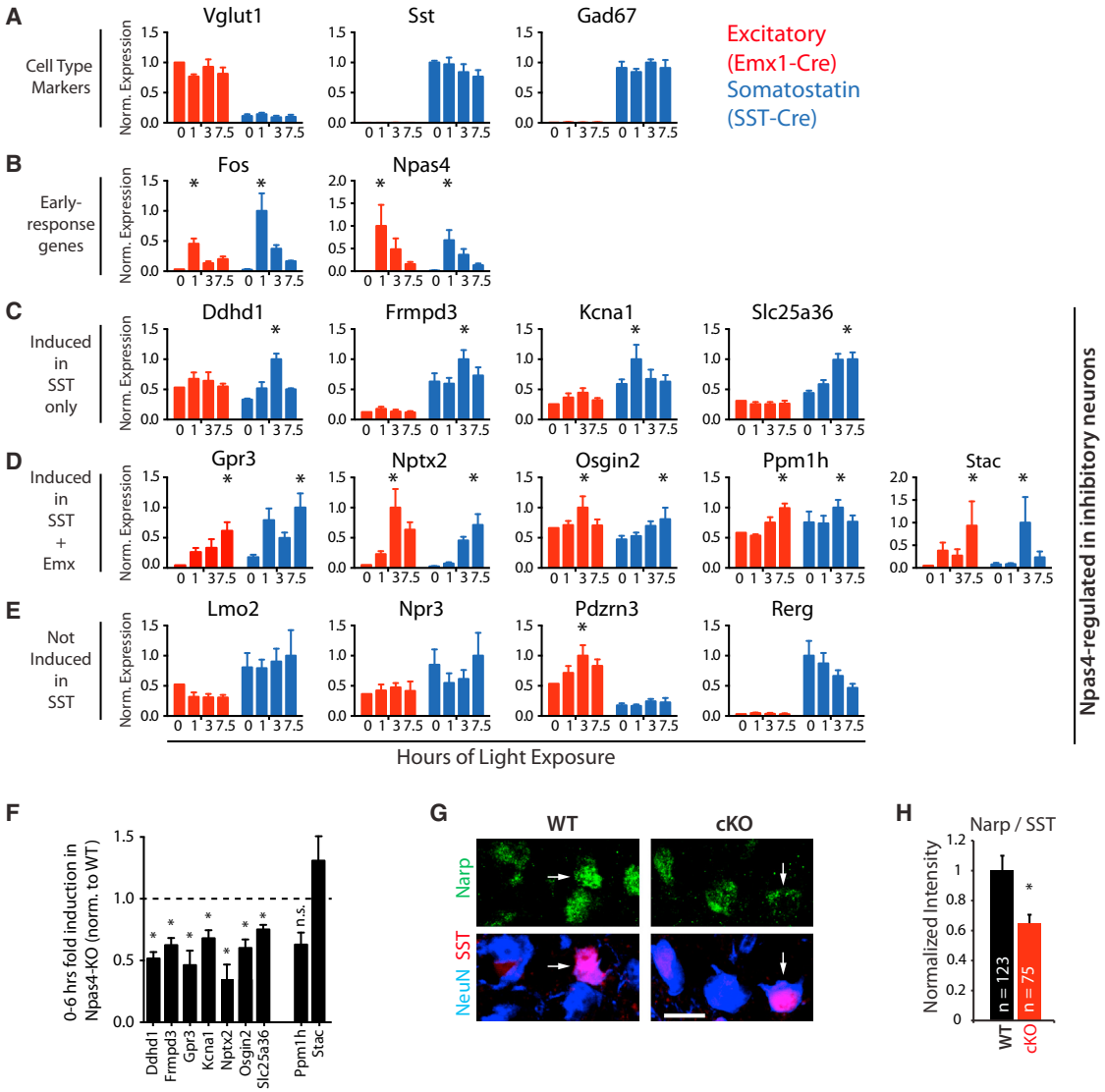

Figure 6. Npas4 Regulates a Cell-Type-Specific Set of Target Genes Induced by Sensory Stimulation in SST Neurons In Vivo

(A–E) Npas4 target genes identified in inhibitory neurons in vitro are induced by sensory experience in a cell-type-specific manner in vivo. Normalized expression of ribosome-associated mRNA from the visual cortex of Emx1-Cre-expressing (red) or SST-Cre-expressing (blue) neurons in dark-housed mice (0 hr) and after light exposure (1, 3, 7.5, hr). Data represent mean + SEM of three bioreps; *, induction defined as a mean >30% increase from the 0 hr time point. (A) Cell-type-specific marker genes. (B) Early-response genes. (C) Npas4 target genes induced selectively in SST neurons. (D) Npas4 target genes induced in both excitatory and SST neurons. (E) Npas4 target genes that are not induced in SST neurons.

(F–H) Experience-induced Npas4 targets in SST neurons are misregulated in the absence of Npas4 in the visual cortex in vivo.

(F) Reduced induction of Npas4 targets in the visual cortex of Npas4-KO mice in response to sensory stimulation. KO and WT mice were dark housed and light exposed, and qPCR analysis was performed on RNA isolated from the visual cortex. Data are represented as mean + SEM of the stimulus-induced fold change in KO mice relative to the normalized fold change observed in WT mice. n = 3 animals per genotype and time point; *, significantly changed induction; $p < 0.05$, two-tailed t test.

(G and H) The levels of Narp, the protein product of the Npas4 target gene *Nptx2*, are reduced in SST neurons lacking Npas4.

(G) Coronal sections from the visual cortex of P11 Npas4 WT and cKO mice lacking Npas4 specifically in SST neurons stained with antibodies directed against Narp (green) and the pan-neuronal marker NeuN (blue) (scale bar, 10 μm).

(H) Quantification of the intensity of Narp immunostaining in SST neuron somata (arrows) in (G). Data are represented as mean + SEM of normalized intensity value across all SST neurons imaged. *, significant difference; $p < 0.005$; Mann-Whitney U test).

See also Figure S6.

at postsynaptic sites of excitatory synapses (*Nptx2*, *Kcna1*) (Hoffman et al., 1997; O'Brien et al., 1999) or are homologous to related molecules (*Frmpd3*) (Lee et al., 2008), suggesting that the function of the Npas4-regulated gene program in SST neurons is to promote excitatory synapse development onto SST neurons.

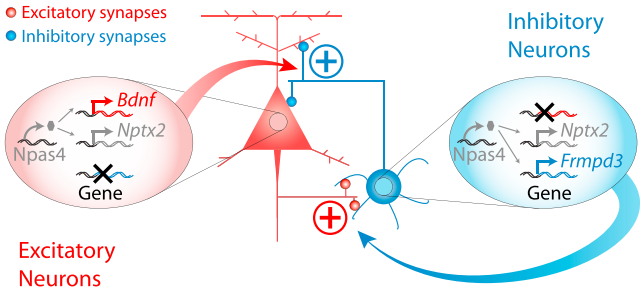

Figure 7. Cell-Type-Specific Functions of Npas4 Are Part of a Circuit-wide Homeostatic Logic to Restrict Excitation

Model demonstrating that the cell-type-specific activity-induced transcriptional programs controlled by Npas4 in excitatory and inhibitory neurons function to regulate different types of synapses to achieve a common homeostatic goal of restricting network activity. In excitatory neurons, Npas4 activates a transcriptional program that consists of late-response genes selectively expressed in excitatory neurons (e.g., *Bdnf*, red) and commonly induced in excitatory and inhibitory neurons (e.g., *Nptx2*, gray). These Npas4 targets function together to promote increased numbers of inhibitory synapses onto excitatory neurons, thereby decreasing circuit activity. In inhibitory neurons, Npas4 activates a transcriptional program consisting of late-response genes selectively expressed in inhibitory neurons (e.g., *Frmpd3*, blue) and genes that are commonly induced by activity in both excitatory and inhibitory neurons (e.g., *Nptx2*, gray). Together, Npas4-regulated late-response genes in inhibitory neurons function to promote increased excitation onto inhibitory neurons, thus increasing GABA release and lowering the overall levels of circuit activity.

DISCUSSION

Activity-Induced Transcriptional Networks in Inhibitory Neurons

Despite the importance of activity-dependent plasticity of inhibition for the development and function of cortical circuits, the study of stimulus-induced events in cortical inhibitory neurons has historically been difficult: widely used protocols for culturing cortical neurons yield cultures that are composed mainly of excitatory neurons, and more recent protocols that allow for the specific isolation of fluorescently labeled inhibitory neurons lack the temporal resolution that is necessary to accurately study transient transcriptional events (Batista-Brito et al., 2008; Okaty et al., 2009). By dissecting mouse embryos at an earlier developmental time point than that used for standard cortical cultures (E14 instead of E16–E18) and by culturing neurons derived from the MGE and from the nascent cortex separately over a prolonged period (~10 days), we were able to circumvent previous limitations and to establish separate cultures of inhibitory and excitatory neurons that proved useful for an initial analysis of acute stimulus-dependent processes in excitatory versus inhibitory neurons. Using this approach, we were able to identify a large number of activity-regulated genes that are specifically induced in inhibitory neurons. Additionally, by profiling of ribosome-associated RNAs, we were able to recapitulate these findings in vivo, showing that many of these genes are activated specifically in inhibitory neurons in response to sensory experience. It seems likely that these newly identified activity-regulated genes underlie the molecular mechanisms by which inhibitory neurons adapt to changes in neural activity. Strikingly, our gene expression analysis led to the finding that several of the best-studied late-response genes in excitatory neurons—including *Bdnf*, *Homer1*, and *Cpg15/Nrn1*—are not induced by neuronal activity in inhibitory neurons. Accordingly, late-response genes that are induced specifically in inhibitory neurons—such as *Igf1*, *Pthlh*, or *Cacng5*—may serve previously unappreciated roles in specifying how inhibitory neurons adjust their synaptic inputs in response to sensory input.

Npas4 Functions in a Cell-Type-Specific Manner according to a Circuit-wide Homeostatic Logic

Our analysis of the activity-induced transcription factor Npas4 revealed that this factor is induced in both excitatory and inhibitory neurons and that it functions in SST neurons to positively regulate the function of excitatory, but not inhibitory, synapses on these neurons. The effect of Npas4 on the development of excitation onto SST neurons is the reciprocal of its role in excitatory neurons, in which it positively regulates the number of inhibitory synapses on excitatory neurons (Lin et al., 2008). The directionality of Npas4's cell-type-specific functions can be understood in the context of neuronal homeostasis (Figure 7): in response to activity, Npas4 is induced in excitatory neurons, where it promotes increased numbers of inhibitory synapses, thereby reducing the activity level of the pyramidal neuron. In SST neurons, elevated activity also induces Npas4, which then acts to promote increased excitation onto the SST neuron. In isolation, this paradoxical form of homeostasis would result in continuously increasing levels of excitation of SST neurons; however, from a circuit-wide perspective, increased excitatory drive to inhibitory neurons should promote increased GABA release and thereby result in decreased net excitation within the local circuit. SST neurons largely receive excitatory input from local cortical afferents, so levels of Npas4 in SST neurons may specifically reflect activity levels in local cortical circuits and could potentially function to fine-tune the amount of feedback inhibition broadcasted by SST neurons throughout the local microcircuit (Silberberg and Markram, 2007). The reciprocal nature of Npas4 function in excitatory and inhibitory neurons demonstrates that key elements of activity-dependent transcriptional pathways are adapted to reflect the distinct function of a particular type of neuron in a neural circuit. Our findings on Npas4 function in SST neurons are consistent with previous reports of strengthening of excitatory synapses onto inhibitory neurons in response to elevated levels of circuit activity (Turrigiano, 2011), supporting the hypothesis that increasing excitation to inhibitory neurons may be a general principle governing the nervous system's response to activity.

Npas4 Activates Cell-Type-Specific Transcriptional Programs of Late-Response Genes

Our findings raise the question of how an activity-induced transcription factor that is ubiquitously expressed in neocortical neurons can activate distinct gene programs in a cell-type-specific manner. The ability of overexpressed Npas4 to induce target genes in a cell-type-specific manner in the absence of neuronal activity indicates that cell-intrinsic mechanisms define the transcriptional outcome of Npas4 activation. Epigenetic chromatin marks on enhancers and promoters have previously been shown to contribute to cell-type-specific gene expression (Whyte et al.,

2013) and thus might also function to define the inducibility of Npas4 target genes in excitatory and inhibitory neurons. Accordingly, while Npas4 acts as a ubiquitous detector of circuit activity, the transcriptional program regulated by Npas4 and thus the specific synapses modulated by Npas4 may be determined by the cohort of accessible regulatory elements in a specific neuronal subtype.

Npas4-Regulated Genes Induced by Sensory Experience in SST Neurons Can Modify Excitatory Synapses

Despite the recent identification of molecules that shape the synaptic connectivity of inhibitory neurons (Fazzari et al., 2010; Sylwestrak and Ghosh, 2012), the molecular mechanisms underlying the plasticity of synaptic inputs to these neurons are still not well understood. Intriguingly, three of the experience-induced Npas4 targets in SST neurons are well suited to regulate excitatory inputs to these cells. *Kcna1* encodes the shaker-like potassium channel Kv1.1, which is expressed in the somatodendritic compartment of neurons and reinforces Hebbian plasticity of excitatory inputs by regulating the electrical properties of dendrites (Hoffman et al., 1997). *Frmpd3* is a yet uncharacterized homolog of the scaffolding molecule *Frmpd4* (i.e., Preso), which associates with PSD-95 and regulates dendritic spine morphogenesis (Lee et al., 2008). Finally, *Nptx2* is an experience-induced Npas4 target gene in both SST neurons and excitatory neurons, the protein product of which (Narp) is present at excitatory synapses on SST neurons (Figure S6). Considering Narp's well-known role in promoting AMPA receptor accumulation and the stabilization of non-spiny excitatory synapses (Koch and Ullian, 2010; O'Brien et al., 1999), these data suggest that Npas4 executes its effect on excitatory synapses in SST neurons at least in part via transcriptional induction of *Nptx2*.

In contrast to our finding that Nptx2/Narp is induced in SST inhibitory neurons, a recent report indicates that Narp is not produced in Parvalbumin-expressing inhibitory neurons (Chang et al., 2010). This suggests that the activity-induced gene expression programs may differ not only between excitatory and inhibitory neurons, but also between distinct subtypes of inhibitory neurons. Supporting this idea, several genes that we identified as activity induced in an Npas4-dependent manner in MGE-derived cultures were not induced by sensory stimulation in SST neurons in the visual cortex; a possible explanation for this observation is that these genes are instead induced by activity in inhibitory neuron subtypes that do not express somatostatin.

In conclusion, our findings indicate that, in excitatory and inhibitory neurons, neuronal activity induces a common set of transcriptional regulators and distinct sets of late-response genes. The early-induced transcriptional regulator Npas4 controls activation of distinct sets of effector genes in inhibitory and excitatory neurons to mediate plasticity responses that are tailored to the specific function of a particular neuronal cell type within a neural circuit. It is intriguing to speculate that this cell-type-specific function of Npas4 may represent a general principle by which common activity-induced transcription factors can activate unique transcriptional programs in different neurons, thereby governing unique cell-type-specific plasticity outcomes in response to activity.

EXPERIMENTAL PROCEDURES

Additional experimental procedures and mouse strains are detailed in the Extended Experimental Procedures.

MGE and CTX Cultures

Cultures were established by dissecting the MGE and CTX of E14 mouse embryos, plating the dissociated cells onto glass bottom dishes (Mattek, Ashland, MA), and maintaining the cultures for 9–11 DIV.

Visual Stimulation

For ICC, P18–P20 mice reared in standard conditions were dark housed for 4 days and subsequently sacrificed either in the dark or after 2.5 hr of light exposure. For RiboTag experiments, 6-week-old mice reared in standard conditions were dark housed for 2 weeks and subsequently sacrificed either in the dark or after 1, 3, or 7.5 hr of light exposure.

RiboTag Analysis

For each time point and genotype, the dissected visual cortices of three animals were pooled. Immunopurification of ribosome-associated RNA was performed as described (Sanz et al., 2009) with minor modifications. Purified RNA was amplified using the Ovation RNA Amplification System V2 (NuGEN, San Carlos, CA), and the resulting cDNA was used for qPCR analysis.

Electrophysiology

Coronal sections were cut from P10–P12 mouse visual cortex in choline dissection media and incubated in artificial cerebral spinal fluid (ACSF). Whole-cell voltage-clamp recordings were performed in ACSF at room temperature from tdTomato-labeled SST neurons identified under fluorescent and DIC optics. mEPSCs were isolated by holding neurons at −70 mV and exposing them to 0.5 μM tetrodotoxin, 50 μM picrotoxin, and 25 μM cyclothiazide and were blocked by application of 25 μM NBQX and 50 μM CPP. mIPSCs were isolated by holding neurons at 0 mV and exposing them to 0.5 μM tetrodotoxin, 25 μM NBQX, and 50 μM CPP and were blocked by 50 μM picrotoxin. Spontaneous EPSCs (sEPSC) were recorded by holding neurons at −70 mV and exposing them to 50 μM picrotoxin, while sIPSCs were recorded by holding neurons at 0 mV and exposing them to 25 μM NBQX and 50 μM CPP. All cells were allowed to stabilize for at least 3 min and were recorded from for at least 25 min following stabilization.

Microarray Analysis and RNA-Seq

Total RNA was collected from MGE or E14 cortical cultures using Trizol reagent following the RNEasy Micro Kit's procedure (QIAGEN, Valencia, CA), and RNA quality was assessed on a 2100 BioAnalyzer (Agilent, Palo Alto, CA). Two independent biological replicates were performed for each microarray experiment in this study. Arrays from all experimental conditions and all replicates of a given condition were normalized to one another using the robust multichip averaging method (RMA normalization) and analyzed using the MATLAB bioinformatics toolbox.

ACCESSION NUMBERS

Microarray and RNA-seq data are available at NCBI GEO (GSE55591).

SUPPLEMENTAL INFORMATION

Supplemental Information includes Extended Experimental Procedures, six figures, and three tables and can be found with this article online at http://dx.doi.org/10.1016/j.cell.2014.03.058.

AUTHOR CONTRIBUTIONS

Experiments were designed by I.S., A.R.M. and M.E.G. Experiments were conducted and analyzed by I.S., A.R.M., H.W.G., J.E.B., C.H.C., C.P.T., and D.A.H. The manuscript was written by I.S., A.R.M., and M.E.G.

ACKNOWLEDGMENTS

We thank F. Polleux and J. De Marchena for help with establishing the MGE cultures, C. Mandel-Brehm and C. Chen for help with electrophysiology experiments, J.M. Gray and A.M. Costa for help with preparing RNA-seq libraries, B.L. Bloodgood for preliminary recordings from MGE cultures, N. Sharma for the lentiviral expression construct of Npas4, E. Griffith and T. Cherry for critical reading of the manuscript, and P. Zhang for managing the mouse colony. This work was funded by fellowships by the Human Frontiers Science Program and the Swiss National Science Foundation (I.S.) and the National Institutes of Health grant NS048276 (M.E.G.).

Received: March 4, 2013
Revised: January 13, 2014
Accepted: March 20, 2014
Published: May 22, 2014

REFERENCES

Batista-Brito, R., Machold, R., Klein, C., and Fishell, G. (2008). Gene expression in cortical interneuron precursors is prescient of their mature function. Cereb. Cortex *18*, 2306–2317.

Bloodgood, B.L., Sharma, N., Browne, H.A., Trepman, A.Z., and Greenberg, M.E. (2013). The activity-dependent transcription factor NPAS4 regulates domain-specific inhibition. Nature *503*, 121–125.

Chang, M.C., Park, J.M., Pelkey, K.A., Grabenstatter, H.L., Xu, D., Linden, D.J., Sutula, T.P., McBain, C.J., and Worley, P.F. (2010). Narp regulates homeostatic scaling of excitatory synapses on parvalbumin-expressing interneurons. Nat. Neurosci. *13*, 1090–1097.

Chattopadhyaya, B., Di Cristo, G., Higashiyama, H., Knott, G.W., Kuhlman, S.J., Welker, E., and Huang, Z.J. (2004). Experience and activity-dependent maturation of perisomatic GABAergic innervation in primary visual cortex during a postnatal critical period. J. Neurosci. *24*, 9598–9611.

Chen, J.L., Lin, W.C., Cha, J.W., So, P.T., Kubota, Y., and Nedivi, E. (2011). Structural basis for the role of inhibition in facilitating adult brain plasticity. Nat. Neurosci. *14*, 587–594.

Coutellier, L., Beraki, S., Ardestani, P.M., Saw, N.L., and Shamloo, M. (2012). Npas4: a neuronal transcription factor with a key role in social and cognitive functions relevant to developmental disorders. PLoS ONE *7*, e46604.

Creyghton, M.P., Cheng, A.W., Welstead, G.G., Kooistra, T., Carey, B.W., Steine, E.J., Hanna, J., Lodato, M.A., Frampton, G.M., Sharp, P.A., et al. (2010). Histone H3K27ac separates active from poised enhancers and predicts developmental state. Proc. Natl. Acad. Sci. USA *107*, 21931–21936.

Fazzari, P., Paternain, A.V., Valiente, M., Pla, R., Luján, R., Lloyd, K., Lerma, J., Marín, O., and Rico, B. (2010). Control of cortical GABA circuitry development by Nrg1 and ErbB4 signalling. Nature *464*, 1376–1380.

Fino, E., and Yuste, R. (2011). Dense inhibitory connectivity in neocortex. Neuron *69*, 1188–1203.

Flavell, S.W., and Greenberg, M.E. (2008). Signaling mechanisms linking neuronal activity to gene expression and plasticity of the nervous system. Annu. Rev. Neurosci. *31*, 563–590.

Garaschuk, O., Linn, J., Eilers, J., and Konnerth, A. (2000). Large-scale oscillatory calcium waves in the immature cortex. Nat. Neurosci. *3*, 452–459.

Hensch, T.K. (2005). Critical period plasticity in local cortical circuits. Nat. Rev. Neurosci. *6*, 877–888.

Hoffman, D.A., Magee, J.C., Colbert, C.M., and Johnston, D. (1997). K+ channel regulation of signal propagation in dendrites of hippocampal pyramidal neurons. Nature *387*, 869–875.

Hong, E.J., McCord, A.E., and Greenberg, M.E. (2008). A biological function for the neuronal activity-dependent component of Bdnf transcription in the development of cortical inhibition. Neuron *60*, 610–624.

Isaacson, J.S., and Scanziani, M. (2011). How inhibition shapes cortical activity. Neuron *72*, 231–243.

Kim, T.-K., Hemberg, M., Gray, J.M., Costa, A.M., Bear, D.M., Wu, J., Harmin, D.A., Laptewicz, M., Barbara-Haley, K., Kuersten, S., et al. (2010). Widespread transcription at neuronal activity-regulated enhancers. Nature *465*, 182–187.

Koch, S.M., and Ullian, E.M. (2010). Neuronal pentraxins mediate silent synapse conversion in the developing visual system. J. Neurosci. *30*, 5404–5414.

Kullmann, D.M., Moreau, A.W., Bakiri, Y., and Nicholson, E. (2012). Plasticity of inhibition. Neuron *75*, 951–962.

Lee, H.W., Choi, J., Shin, H., Kim, K., Yang, J., Na, M., Choi, S.Y., Kang, G.B., Eom, S.H., Kim, H., and Kim, E. (2008). Preso, a novel PSD-95-interacting FERM and PDZ domain protein that regulates dendritic spine morphogenesis. J. Neurosci. *28*, 14546–14556.

Lewis, D.A., Hashimoto, T., and Volk, D.W. (2005). Cortical inhibitory neurons and schizophrenia. Nat. Rev. Neurosci. *6*, 312–324.

Lin, Y., Bloodgood, B.L., Hauser, J.L., Lapan, A.D., Koon, A.C., Kim, T.-K., Hu, L.S., Malik, A.N., and Greenberg, M.E. (2008). Activity-dependent regulation of inhibitory synapse development by Npas4. Nature *455*, 1198–1204.

Markram, H., Toledo-Rodriguez, M., Wang, Y., Gupta, A., Silberberg, G., and Wu, C. (2004). Interneurons of the neocortical inhibitory system. Nat. Rev. Neurosci. *5*, 793–807.

Maya-Vetencourt, J.F., Tiraboschi, E., Greco, D., Restani, L., Cerri, C., Auvinen, P., Maffei, L., and Castrén, E. (2012). Experience-dependent expression of NPAS4 regulates plasticity in adult visual cortex. J. Physiol. *590*, 4777–4787.

O'Brien, R.J., Xu, D., Petralia, R.S., Steward, O., Huganir, R.L., and Worley, P. (1999). Synaptic clustering of AMPA receptors by the extracellular immediate-early gene product Narp. Neuron *23*, 309–323.

Okaty, B.W., Miller, M.N., Sugino, K., Hempel, C.M., and Nelson, S.B. (2009). Transcriptional and electrophysiological maturation of neocortical fast-spiking GABAergic interneurons. J. Neurosci. *29*, 7040–7052.

Ploski, J.E., Monsey, M.S., Nguyen, T., DiLeone, R.J., and Schafe, G.E. (2011). The neuronal PAS domain protein 4 (Npas4) is required for new and reactivated fear memories. PLoS ONE *6*, e23760.

Ramamoorthi, K., Fropf, R., Belfort, G.M., Fitzmaurice, H.L., McKinney, R.M., Neve, R.L., Otto, T., and Lin, Y. (2011). Npas4 regulates a transcriptional program in CA3 required for contextual memory formation. Science *334*, 1669–1675.

Rudy, B., Fishell, G., Lee, S., and Hjerling-Leffler, J. (2011). Three groups of interneurons account for nearly 100% of neocortical GABAergic neurons. Dev. Neurobiol. *71*, 45–61.

Sanz, E., Yang, L., Su, T., Morris, D.R., McKnight, G.S., and Amieux, P.S. (2009). Cell-type-specific isolation of ribosome-associated mRNA from complex tissues. Proc. Natl. Acad. Sci. USA *106*, 13939–13944.

Silberberg, G., and Markram, H. (2007). Disynaptic inhibition between neocortical pyramidal cells mediated by Martinotti cells. Neuron *53*, 735–746.

Somogyi, P., and Klausberger, T. (2005). Defined types of cortical interneurone structure space and spike timing in the hippocampus. J. Physiol. *562*, 9–26.

Sylwestrak, E.L., and Ghosh, A. (2012). Elfn1 regulates target-specific release probability at CA1-interneuron synapses. Science *338*, 536–540.

Turrigiano, G. (2011). Too many cooks? Intrinsic and synaptic homeostatic mechanisms in cortical circuit refinement. Annu. Rev. Neurosci. *34*, 89–103.

Whyte, W.A., Orlando, D.A., Hnisz, D., Abraham, B.J., Lin, C.Y., Kagey, M.H., Rahl, P.B., Lee, T.I., and Young, R.A. (2013). Master transcription factors and mediator establish super-enhancers at key cell identity genes. Cell *153*, 307–319.

Wiesel, T.N., and Hubel, D.H. (1963). Single-cell responses in striate cortex of kittens deprived of vision in one eye. J. Neurophysiol. *26*, 1003–1017.

Wonders, C.P., and Anderson, S.A. (2006). The origin and specification of cortical interneurons. Nat. Rev. Neurosci. *7*, 687–696.

EXTENDED EXPERIMENTAL PROCEDURES

Neuronal Cell Culture

For immunocytochemistry and synaptic puncta quantification experiments, mixed cortical cultures were prepared from E16.5 mouse embryos as described (Xia et al., 1996). Briefly, $1.25x10^5$ neurons per well were plated on a glial support layer on glass coverslips coated with Poly-D-Lysine (20 μg/mL) and Laminin (3.4 μg/mL) in 24-well dishes. For synaptic puncta quantification experiments after Npas4-OE, $7.5x10^4$/well astrocytes were added 1 day after lentiviral infection. Cultures were maintained in Neurobasal medium supplemented with B27 (Invitrogen), 1 mM L-glutamine, and 100 U/mL penicillin/streptomycin, and one third of the media in each well was replaced every other day. Cultures were maintained for 9 days (Npas4-OE experiments) or 2 weeks (all other experiments) in vitro before fixation.

MGE-derived and E14 cortical cultures were established by dissecting E14 embryos as previously described (Bortone and Polleux, 2009) and maintained for 9-11 DIV in Neurobasal medium supplemented with B27 (Invitrogen), 1 mM L-glutamine, and 100 U/mL penicillin/streptomycin. E14 MGEs were dissociated into a single cell suspension (Polleux and Ghosh, 2002) and plated onto glass bottom petri dishes (MatTek; $1x10^5$ cells onto 35/14 mm dishes or $1x10^6$ cells onto 60/30 mm dishes) coated with Poly-D-Lysine (20 μg/mL) and Laminin (3.4 μg/mL). After one week in culture, one third of the medium was replaced every other day. For E14 cortical cultures, cortices were dissociated and plated at a density of $1x10^6$ single cells per well on 6-well plates coated with poly-D-lysine (20 μg/mL) and laminin (3.4 μg/mL) and one third of the media in each well was replaced every other day.

For KCl-mediated depolarization of neurons, neuronal cultures were treated overnight with 1 μM TTX and 100 μM AP-5 to silence spontaneous activity prior to stimulation. Neurons were depolarized with 55 mM extracellular KCl as described (Tao et al., 1998) and lysed at the indicated time point. For glutamate-stimulation, neuronal cultures were treated overnight with 1 μM TTX and 100 μM AP-5 and 40 μM CNQX 1 hr prior to stimulation with 20 μM glutamate.

Lentiviral supernatants were prepared as described (Tiscornia et al., 2006) and neuronal cultures were infected at DIV4 with fresh undiluted viral supernatant for 4 hr. After infection, the cultures were washed twice in plain Neurobasal medium after which the conditioned medium was returned to the dish and the cultures were continued to be maintained as described.

Western Blot Analysis

DIV7 E16.5 mixed cortical or DIV9 E14 MGE cultures were placed on ice, washed 1x with cold PBS, and immediately exposed to boiling sample buffer (75 mM Tris HCl pH 6.8, 15% glycerol, 3% SDS, 7.5% β-Mercaptoethanol). Samples were boiled for five minutes and centrifuged at maximum speed for 5 min. The supernatant was resolved by SDS-PAGE, transferred to nitrocellulose, and immunoblotted. Protein levels were visualized by chemiluminescence. Antibodies used were Rb α-c-Fos (Santa Cruz SC-52 1:200), Rb α-Npas4 (in house, 1:2,000), Ms α-Tuj-1 (Millipore MAB1637 1:10,000), Rb α-Gad65/67 (Millipore AB1511 1:10,000), Rb α-Tbr1 (Abcam ab31940 1:500).

Cloning of Lentiviral Expression Vectors

cDNA cloning of lentiviral expression constructs was done with standard cloning techniques. For pFUW-Npas4, full length mouse Npas4 cDNA was cloned into pFUGW (Addgene plasmid #14883) by replacing EGFP, and pFUW-Flex-Npas4-2A-EGFP and pFUW-Flex-2A-EGFP were cloned by inserting the respective fragments into pFUW. The integrity of all cloned constructs was validated by DNA sequencing.

Immunocytochemistry

Neurons were fixed in 4% PFA and 1% sucrose in PBS for 8 min at room temperature, then washed in PBS 3x20 min. Coverslips were blocked for 1 hr (5% Normal Goat Serum, 0.1% Triton X-100 in PBS) then incubated in primary antibody in block overnight at 4°C. Coverslips were washed 4x10 min in PBS and incubated in secondary antibody in block for one hour at RT away from light. Coverslips were washed 4x10 min in PBS and 1x in distilled water before being mounted in fluoromount-G (SouthernBiotech) and stored at 4°C before imaging. Primary antibodies used were: Rb α-Fos (Santa Cruz sc-52, 1:500), Rb α-Npas4 (in house, 1:500), Rb α-Somatostatin (Millipore AB5494 1:500), Rat α-Somatostatin (Millipore AB354 1:100), Sheep α-NPY (Millipore AB1583 1:200), Ms α-Calretinin (Swant 6B3 1:500), Ms α-Calbindin (Swant 300 1:500), Goat α-Parvalbumin (Swant PVG 214 1:200), Rb α-Parvalbumin (Swant PV25 1:500), Ms α-GAD67 (Millipore MAB5406 1:500), Rb α-Narp (Novus Biologicals 32250002 1:1000). Secondary antibodies were Alexa Fluors (Invitrogen) used at a concentration of 1:500.

RNA Isolation, Reverse Transcription, qPCR Analysis

Total RNA was extracted with Trizol reagent following the RNEasy Micro Kit's procedure (QIAGEN, Valencia, CA) and RNA quality was assessed on a 2100 BioAnalyzer (Agilent, Palo Alto, CA). RNA was reverse transcribed with the High Capacity cDNA Reverse Transcription kit (Life Technologies). Real-time quantitative PCR reactions were performed on the LightCycler 480 system (Roche) with LightCycler 480 SYBR Green I Master. Reactions were run in duplicates or triplicates and beta-Actin (*ActB*) or Tubulin beta 3 (*Tubb3*) levels were used as an endogenous control for normalization using the ΔΔCt method (Livak and Schmittgen, 2001). Real-time PCR primers were designed using the Universal ProbeLibrary (Roche) and listed in Table S1. Data were normalized to the maximally expressed sample in each biological replicate, and data in figures represent the mean and SEM of 3-4 biological replicates.

Microarray Analysis and RNA-Seq

Total RNA was collected from MGE or E14 cortical cultures using Trizol reagent following the RNEasy Micro Kit's procedure (QIAGEN, Valencia, CA) and RNA quality was assessed on a 2100 BioAnalyzer (Agilent, Palo Alto, CA). For oligonucleotide microarray hybridization, 100 ng of total RNA were amplified with the Ovation RNA Amplification System V2 (NuGEN, San Carlos, CA) and the resulting cDNA was labeled, fragmented and hybridized to Affymetrix Mouse Genome 430 2.0 arrays. Preparation of cDNA and hybridization of cDNA to microarrays was conducted in the Microarray core facility at Dana-Farber Cancer Institute, and all microarrays passed standard Affymetrix quality control tests. Two independent biological replicates were performed for each microarray experiment in this study. Arrays from all experimental conditions and all replicates of a given condition were normalized to one another using the robust multichip averaging method (RMA normalization) using the MATLAB bioinformatics toolbox (Bolstad et al., 2003).

To identify well-expressed probe sets, an absolute expression threshold was set at four times the highest signal from the Npas4 probe set in the Npas4 knockout condition. Probe sets were considered for further analysis if the probe set intensity in one or more experimental conditions was greater than this threshold in 2 out of 2 biological replicates. Approximately 40% of probe sets passed this filter; importantly, repetition of our analysis of cell type-specific inducible genes using an expression threshold half as stringent changed the number of identified genes but did not alter the major conclusions of our analysis.

Fold-changes were calculated in each experiment by dividing the probe set intensity from either the 1 or 6 hr sample by the intensity from the 0 hr sample. Probe sets were considered to be induced by membrane depolarization if their fold-induction was equal to or greater than 2 at a given time point in 2 out of 2 biological replicates. The 2-fold induction threshold was chosen based on prior studies of activity-regulated genes, and quantitative RT-PCR experiments confirmed that changes 2-fold or greater were accurately reported by the arrays (Flavell et al., 2008).

Using this cutoff, we identified 1077 inducible probe sets; these probe sets were categorized into six distinct groups: maximally induced at 1 hr in MGE cultures only, E14 CTX cultures only, or in both cultures, and maximally induced at 6 hr in MGE cultures only, E14 CTX cultures only, or in both cultures. Probe sets were sorted into one of these six categories on the basis of three criteria: 1) expression, 2) differential induction, and 3) kinetics of induction. First, the fold-induction for every probe set was calculated as described for each time point in both cultures, yielding four values: fold-induction of a probe set in the MGE cultures at 1h and 6h, and in E14 CTX cultures at 1h and 6h. Next, the expression filter was applied to these four values; for each fold-induction, if the probe set intensity at the induced time point (e.g., non-0h time point) was below the expression cutoff, then the fold-induction for that time point was set to 0. This filter removed large fold-changes resulting from technical noise prevalent in the most poorly expressed probe sets.

Next, a filter was applied to each probe set to determine whether it was similarly or differentially induced between MGE and E14 CTX cultures at each time point. If the fold-induction of a probe set in both cultures at a given time point fell on the same side of the 2-fold induction threshold (either above or below), then they were determined to respond similarly to membrane depolarization at that time point. If, at a given time point, the fold-induction of a probe set in one culture was above threshold, but its fold-induction in the other culture was below threshold, then they were scored as responding differently to membrane depolarization. To avoid potential threshold effects, a secondary filter was applied to account for experimental noise around the 2-fold threshold: for each probe set that was induced above the 2-fold threshold in only one culture type, but not induced higher than 3-fold (e.g., near our threshold), we asked if the fold-inductions of that probe set in MGE and E14 CTX cultures were within 25% of the magnitude of the higher fold-induction. If so, this probe set was classified as induced in both cultures. This strategy avoided a potential source of error resulting from application of a strict threshold for fold-induction. Finally, probe sets were sorted into either the one or six hour induction category based on the kinetics with which they were maximally induced. A small number of probe sets were induced in both MGE and E14 CTX cultures but had distinct kinetics, peaking at one hour in MGE cultures and six hours in E14 CTX cultures.

Multiple probe sets targeting the same gene were not removed from the data set, meaning that reports of probe set numbers may include multiple probe sets identifying the same gene. However, the discussion of the number of transcriptional regulators induced rapidly by neuronal activity refers to the number of genes encoding transcriptional regulators, not the number of probe sets directed against them. Rarely, probe sets against the same gene fell into different cell-type-specific or kinetics categories. These discrepancies were not reconciled since we hypothesized that they may represent cell-type-specific splicing or exon usage.

Construction of RNA-Seq libraries and RNA-Seq analysis were performed as described (Kim et al., 2010). RNA was collected as described above for the microarray analysis. RNA-Seq libraries for whole transcriptome sequencing were prepared using the SOLiD Whole Transcriptome Analysis Kit (Life Sciences) and completed libraries were validated by qPCR. SOLiD sequencing of RNA-Seq libraries was performed on a SOLiD instrument (3.0 version) with 35-bp reads according to manufacturer's instructions (Life Technologies). All experiments were performed on full sequencing slides with barcodes used to distinguish up to 16 sequencing libraries on a slide. RNA-Seq was performed to a depth of $\sim 10 \times 10^6$ clean reads per sample. Mapping of RNA-Seq reads and subsequent analysis of read-densities across all UCSC annotated genes were performed as described (Kim et al., 2010).

Visual Stimulation

For Npas4 immunostaining experiments, P18-20 mice reared in a standard light cycle were transferred into constant darkness for four days. Animals in the light-exposed condition were subsequently exposed to light for 2.5 hr before being sacrificed, while animals in the dark housed condition were anesthetized in the dark and their eyes were covered before being sacrificed. For RiboTag experiments, six-week-old mice reared in a standard light cycle were housed in constant darkness for two weeks. Animals in the

light-exposed condition were subsequently exposed to light for 1, 3, or 7.5 hr before being sacrificed. Animals in the dark-housed condition were sacrificed in the dark; after being sacrificed, their eyes were enucleated before dissection of the visual cortex in the light.

Perfusions and Immunohistochemistry

Animals were anesthetized with 300 μl 10% ketamine and 1% xylazine in PBS by intraperitoneal injection. When animals were fully anaesthetized, as judged by lack of response to tail pinch, animals were transcardially perfused with ice cold PBS for one minute followed by six minutes of cold 4% PFA, 1% sucrose in PBS. Brains were dissected out and postfixed for one hour at 4°C, followed by 3x30 min washes in cold PBS, and cryoprotection overnight in 20% sucrose in PBS at 4°C. For Narp immunostaining experiments, brains were postfixed in 1% PFA at 4°C for two days. The following day, brains were placed in tissue freezing medium (Triangle Biomedical Sciences) and frozen on dry ice and stored at −80°C. Brains were subsequently cryosectioned using a Leica CM1950 cryostat at a thickness of 20 μm. Brains from different experimental conditions were placed on the same slide to minimize variation. After cryosectioning, slides were either stained immediately or stored at −20°C for up to six months. Brain sections were initially blocked for one hour (0.3% Triton X-100, 0.2% Tween-20, 3% Normal Goat Serum and 3% BSA), followed by incubation of primary antibody overnight at 4°C in block. The next day, brains were washed 3x15 min in PBS-T (PBS with 0.25% Triton X-100), incubated with secondary antibodies and DAPI in block for 1 hr at RT, then washed 3x15 min in PBS-T, once in distilled water, and mounted in fluoromount-G (SouthernBiotech). Primary and secondary antibodies were the same as described for use in immunocytochemistry, and all were used at concentrations of 1:1000.

Synaptic Puncta Staining and Quantification of Synapse Density

Cultured neurons were washed with PBS and fixed with 4% paraformaldehyde and 1% sucrose in PBS for 8 min at room temperature. Following PBS washes, neurons were blocked in 1x GDB (0.1% gelatin, 0.3% Triton X-100, 4.2% 0.4 M phosphate buffer, 9% 5 M NaCl), incubated with the primary antibody in 1x GDB overnight at 4°C, washed 4 × 10 min in PBS, and then incubated with the secondary antibody in 1x GDB for 1 hr at room temperature. Neurons were then washed 4x10 min in PBS and once in distilled water before being mounted in Fluoromount-G (SouthernBiotech). The following primary antibodies were all used at a dilution of 1:250: Ms α-PSD-95 (Millipore MAB1596), Rb α-Synapsin-1 (Millipore, AB1543), Ms α-GABAAR β2/3 (MAB341), Ms α-Vglut-1 (Millipore MAB5905), Rb α-GluR1 (Millipore AB1504), Rb α-GABAAR γ2 (Millipore AB5559), Rb α-Gad65 (Millipore AB5082), Ms α-Vgat (Synaptic Systems 131 011). Alexa Fluor secondary antibodies (Invitrogen) were used at a concentration of 1:250.

Images were acquired using a Zeiss Axio Imager microscope with a 63x objective with the use of an apotome. Within each set of synaptic markers in a given experiment, all images were acquired with identical exposure times and apotome settings. Settings were selected such that no pixels were beyond the range of the detector. For each neuron, a Z-stack of 6-8 sections with a step size of 0.5 μm was collected, and a maximal intensity projection was created and used for analysis. Neurons were analyzed blind to genotype or experimental condition. Custom ImageJ macros were used to remove the somatic region of the labeled SST neuron from the image and to create a mask of the tdTomato-labeled dendrites. A custom MATLAB program was used to determine synapse density. Briefly, for each channel in each experiment, the mean pixel intensity was determined, and an intensity threshold was set at three standard deviations above the mean. Similar results were obtained using thresholds of either 2 or 4 standard deviations above the mean. Each channel of each image was masked and binarized, and the intersection of all three channels was determined. Connected components greater than three pixels in size were identified and counted. Synapse density for each neuron was determined by dividing the number of triple overlapping co-clusters by the total area of the dendrites. Mean values for each biological replicate were determined from at least 15 neurons imaged from multiple coverslips. Because absolute values of synapse density vary between biological replicates, for each set of synaptic markers in each biological replicate, the control group mean was set to 1 and synapse density in other groups was normalized to this value. Normalized mean data were used to analyze significance by ANOVA using Graphpad Prism 6.0. Data represent the mean and SEM of three independent biological replicates, with the total number of neurons analyzed across three biological replicates indicated in the figures.

Electrophysiology

Coronal sections (300 μm) were cut from P10-12 mouse visual cortex using a Leica VT1000S vibratome in ice-cold choline dissection media (25 mM $NaHCO_3$, 1.25 mM NaH_2PO_4, 2.5 mM KCl, 7 mM $MgCl_2$, 25 mM glucose, 0.5 mM $CaCl_2$, 110 mM choline chloride, 11.6 mM ascorbic acid, 3.1 mM pyruvic acid). Slices were incubated in artificial cerebral spinal fluid (ACSF, contains 127 mM NaCl, 25 mM $NaHCO_3$, 1.25 mM NaH_2PO_4, 2.5 mM KCl, 2 mM $CaCl_2$, 1 mM $MgCl_2$, 25 mM glucose) at 32°C for 30 min immediately after cutting, and subsequently at room temperature. All solutions were saturated with 95% O_2/5% CO_2, and slices were used within 6 hr of preparation. Whole-cell voltage-clamp recordings were performed in ACSF at room temperature from tdTomato-labeled SST neurons identified under fluorescent and DIC optics. Recording pipettes were pulled from borosilicate glass capillary tubing with filaments using a P-1000 micropipette puller (Sutter Instruments) and yielded tips of 2-5 MΩ resistance. All experiments were recorded with pipettes filled with 135 mM Cesium Methanesulfonate, 15 mM HEPES, 0.5 mM EGTA, 5 mM TEA-Cl, 1 mM MgCl2, 0.16 mM CaCl2, 2 mM Mg-ATP, 0.3 mM Na-GTP, 10 mM Phosphocreatine (Tris), and 2 mM QX-314-Cl. Osmolarity and pH were adjusted to 310 mOsm and 7.3 with Millipore water and CsOH, respectively. Occasionally 0.5% Neurobiotin (Vector Labs) or Alexa Hydrazide 488 (Invitrogen) was included in the internal solution to visualize neurons. Recordings were sampled at 20 kHz and filtered at 5 kHz.

mEPSCs were isolated by holding neurons at −70 mV and exposing them to 0.5 μM tetrodotoxin, 50 μM picrotoxin and 25 μM cyclothiazide and were blocked by application of 25 μM NBQX and 50 μM CPP. mIPSCs were isolated by holding neurons at 0 mV and exposing them to 0.5 μM tetrodotoxin, 25 μM NBQX, and 50 μM CPP and were blocked by 50 μM picrotoxin. Spontaneous EPSCs (sEPSC) were recorded by holding neurons at −70 mV and exposing them to 50 μM picrotoxin, while sIPSCs were recorded by holding neurons at 0 mV and exposing them to 25 μM NBQX and 50 μM CPP. All cells were allowed to stabilize for at least three minutes and were recorded from for at least 25 min following stabilization.

Data were analyzed using Axograph X. Events were identified using a variable amplitude template-based strategy as described (Clements and Bekkers, 1997). Templates for each event type were defined as follows. mEPSC: 0.25 ms rise time, 3 ms decay τ, amplitude threshold of −3xSD local noise. mIPSC: 1 ms rise time, 50 ms decay τ, amplitude threshold of 2.5xSD local noise. Local noise was determined by calculating the standard deviation of the current in a 5 ms window before event rise onset. Template lengths were extended 25 ms after rise onset in the case of mEPSCs and 50 ms after rise onset in the case of mIPSCs. Events were discarded if they were larger than 100 pA or had a rise time outside the range of 0-3 ms for mEPSCs or 0-10 ms for mIPSCs. Statistical significance for all recorded parameters between genotypes was evaluated using a Mann-Whitney U-test on the mean values from individual neurons in a given experiment. Cumulative distributions of inter-event interval and amplitude were made for every cell, and presented as the mean ± SEM distribution of the distribution from each cell in a given experiment. Cumulative distribution plots are not shown for mIPSCs because the mIPSCs onto SST neurons were so infrequent at P10-12 that despite recording for 40 min, we often sampled less than 100 events, too few to to reasonably estimate the distribution. Cells were discarded if they had a series resistance larger than 20 MΩ during the recordings, if average noise RMS was over 3.5 pA, or if baseline drifted more than 30% over the course of recording.

Morphometric Reconstruction and Sholl Analysis

For Sholl analysis performed on cultured neurons, the tdTomato signal was isolated by applying a user-defined threshold and fed into a custom MATLAB program that analyzed the resulting image. Mean and SEM were determined from every neuron imaged across every biological replicate of the synapse staining experiments.

For morphological reconstruction of somatostatin neurons in vivo, acute coronal slices were prepared as described, and neurons were identified by tdTomato expression reporting SST-Cre activation. SST neurons were intracellularly filled using a patch pipette of 2-3.5 MΩ resistance with an internal solution containing 0.5% neurobiotin (Vector Labs) and allowed to dialyze for 40 min. After careful removal of the pipette from the cell, the slice was immediately fixed in 4% PFA in 0.1 M phosphate buffer (PB) with 0.2% picric acid overnight at 4°C. The next day, the slices were washed 3x20 min in 0.1M PB, then cryoprotected in 30% sucrose in 0.25 M PB, frozen in tissue freezing medium (Triangle Biomedical Sciences) on dry ice and stored at −80°C. Slices were defrosted in 0.1 M PB and washed 3x20 min in 0.1 M PB to remove excess freezing medium. Slices were treated with 1% hydrogen peroxide in 0.1M PB for 30 min, washed 3x20 min in PBS, then treated with 0.4% Triton X-100 for 1 hr. Following Triton treatment, slices were incubated with AB reagent (Vector Labs) prepared according to manufacturer's instructions for 2 hr. Slices were rinsed 3x20 min in PBS, then exposed to ImmPACT DAB (Vector Labs) prepared according to manufacturer's instructions until slices turned light brown. Slices were immediately transferred to PBS and washed 3x20 min in PBS. Finally, slices were dehydrated in a series of brief washes of increasing ethanol concentrations and then washed twice in Xylene before being mounted in Permount (Fisher Scientific). Cells were visualized using a Nikon 80i upright microscope with a 100x Nikon Plan Fluor oil, 1.3 Na objective and were traced using Neurolucida (MBF Bioscience). Sholl analysis was performed on Neurolucida reconstructions using Neurolucida Explorer.

Cell Counting Experiments

For cell counting experiments, cultured neurons or brain sections were imaged using a Zeiss Axio Imager microscope with either a 10x objective or a 20x objective with an apotome. In all cases, image exposures were set to ensure less than 0.4% of the pixels were saturated, and exposures were kept constant throughout a given experiment for each channel. Custom ImageJ and MATLAB macros were used to quantify the fraction of a specific type of neuron that stained positive for a transcription factor. Briefly, for each image, a threshold for each channel was determined based on multiple user-defined negative regions. Channels were thresholded and binarized, and a mask of each channel was created. The total number of nuclei in an image was determined by counting the number of connected components greater than 6 pixels in size in the DAPI channel, while the number of cells positive for a given marker was determined by taking the logical AND of the DAPI and cell type marker channel masks and counting the number of connected components greater than 4 pixels in size. Finally, the number of cells positive for both a cell type marker and a transcription factor was determined by counting the number of components greater than 4 pixels in size in the triple overlap of the masks of each of the three channels. These counts and the total area of the image or a region of interest were used to calculate the reported densities or percentages. For each experiment, at least three separate images were used to determine mean values for each biological replicate, and at least three biological replicates (animals or cultures) were used to determine mean and SEM of reported values.

Identification of Npas4-Regulated Genes in MGE and CTX Cultures

Microarrays from membrane depolarized MGE cultures prepared from Npas4 KO mice were performed and normalized in parallel with the experiments described above. To analyze the transcriptional program controlled by Npas4 in MGE-derived neurons, both the 0-1 hr and 0-6 hr fold-inductions were calculated from WT and Npas4 KO cultures as described above and plotted against

each other. We set stringent criteria designed to detect genes most highly regulated by Npas4 and to exclude false positives. High-confidence Npas4-regulated genes were found on the basis of three criteria: 1) The 0-6 hr fold induction in WT MGE cultures should be 2-fold or greater in both biological replicates, 2) the expression levels in both biological replicates of the WT MGE 6 hr time point should be above expression threshold, 3) the probe set intensity should be decreased by $\geq$ 35% at the six hour time point in the Npas4 KO. Identification of Npas4-regulated genes in CTX cultures was done using the same criteria for CTX cultures. Genes that satisfied these criteria in both MGE and CTX cultures were classified as Npas4 targets in both cultures.

Identification of Npas4-Binding Sites near Regulated Genes

Available ChIP-Seq data sets from membrane depolarized E16.5 cortical cultures (Kim et al., 2010) were combined with RNA-Seq performed from membrane depolarized MGE-derived cultures to identify sites of Npas4 binding at DNA regulatory regions (enhancers and promoters) in the vicinity of the genomic locus of Npas4 target genes. Activity-regulated enhancers were defined as described (Kim et al., 2010) by the presence of inducible CBP binding peaks and the presence of H3K4me1 signal. Enhancers were assigned to a given Npas4-regulated gene if the enhancer was within 50 kb upstream of the RNA transcriptional start site, or if the enhancer was located in the intronic region of the gene. The site of RNA transcription initiation and the presence of H3K4me3 and RNA Polymerase II signal defined promoters. Except in rare cases (e.g., *Frmpd3*), these criteria defined promoters that were consistent with Refseq annotated genes. For each Npas4-regulated gene, the number of upstream and intragenic enhancers inducibly bound by Npas4 and the presence or absence of an inducible Npas4 binding peak at the promoter were reported.

H3K27Ac Chromatin Immunoprecipitation

Chromatin immunoprecipitation (ChIP) was performed as previously described (Ebert et al., 2013; Kim et al., 2010) with modifications to facilitate isolation of chromatin from small numbers of cells: DIV10 E14 cortical or E14 MGE cultures were silenced overnight and cells were either left untreated or membrane depolarized for 2 hr. Following depolarization, media was removed and the cells were fixed for 10 min at room temperature in 4 ml of crosslinking buffer (10 mM HEPES pH 7.5, 100 mM NaCl, 1 mM EDTA, 1 mM EGTA, 1% formaldehyde), followed by addition of glycine to 125 mM for 5 min. Samples were washed twice with ice-cold PBS containing PMSF, and cells were lysed and scraped from the plates in L1 lysis buffer (50 mM HEPES pH 7.5, 140 mM NaCl, 1 mM EDTA, 1 mM EGTA, 0.25% Triton X-100, 0.5% NP-40, 10% glycerol, 1X Roche complete protease inhibitors, 10 mM Sodium Butyrate). Nuclei were isolated by sequential resuspension and centrifugation (10 min, 700Xg) in L1 buffer, and L2 buffer (10 mM Tris pH 8.0, 200 mM NaCl, 1X Roche complete EDTA-free protease inhibitors, 10 mM Sodium Butyrate), then resuspended in L3 buffer (10 mM Tris pH 8.0, 1mM EDTA, 1 mM EGTA, 1X Roche complete EDTA-free protease inhibitors, 10 mM Sodium Butyrate) and frozen until fragmentation was performed. To fragment chromatin, nuclei from 1-2 million cultured cells were thawed and sonicated in 1 ml L3 + 0.15% SDS using a Covaris S2 sonicator (8 min, 5% duty cycle, power level 4, 200 cycles per burst). Samples were adjusted to 1.5 ml in SDS-ChIP Buffer (10 mM Tris pH 8.0, 0.1% SDS,1% Triton X-100, 150 mM NaCl, 1 mM EDTA, 0.3 mM EGTA, 1X Roche complete EDTA-free protease inhibitors, 10 mM Sodium Butyrate), precleared with protein A Dynabeads (Invitrogen, Carlsbad CA), "Input" samples were taken, and immunoprecipitation was carried out overnight rotating at 4°C using 0.12 μg of anti-Histone H3 Lysine 27 Acetyl antibody (Abcam ab4729) coupled to protein A Dynabeads. The supernatant was then removed and beads were washed at 4°C twice with low salt wash buffer (0.1% SDS, 20 mM Tris pH 8.0, 1% Triton X-100, 150 mM NaCl, 2 mM EDTA), twice with high salt wash buffer (0.1% SDS, 20 mM Tris pH 8.0, 1% Triton X-100, 500 mM NaCl, 2 mM EDTA), twice with LiCl wash buffer (1% NaDOC, 10 mM Tris pH 8.0, 1% NP40, 250 mM LiCl, 1 mM EDTA), and once with TE. DNA was eluted by incubation for 30 min at 65°C in TE + 1% SDS. Input and immunoprecipitated DNA were decrosslinked for 12-16 hr at 65°C, treated with RNase (10 μg RNase A, 0.5-1 hr, 37°C) and Proteinase K (280 μg, 2 hr, 55°C), phenol/chloroform extracted, and DNA was isolated using QIAGEN PCR purification columns (QIAGEN, Valencia CA). To check fragmentation, DNA was isolated from the supernatant of the IP and run on a 2% agarose gel. Similar fragmentation was confirmed for all experiments, with ~80% of the DNA appearing as a smear approximately 100-500 bp in length. Quantitative PCR analysis was carried out using the StepOnePlus qPCR system and Power SYBR Green mix (Life technologies, Beverly, MA); the sequences of the primers used for qPCR are listed in Table S2. A "fraction of input" value for each amplicon was determined by comparing the average threshold cycle of the immunoprecipitated DNA to a standard curve generated using serial dilutions of the input DNA and interpolating the amount of IP DNA relative to this input curve. To determine fold enrichment above background for each site, the fraction of input values for each target amplicon in each sample was divided by the average fraction of input signal in that sample for two amplicons targeting negative regions of the genome known to be devoid of histone acetylation (*Bdnf* Upstream and Major Satellites). Experiments were performed in quadruplicates and averages and SEM were calculated.

RiboTag Analysis

Immunoprecipitation and purification of ribosomally associated RNA was performed essentially as described (Sanz et al., 2009) with minor modifications: lysis of the samples was performed in the presence 10 mM Ribonucleoside Vanadyl Complex (NEB, Ipswich, MA) instead of Heparin and immunoprecipitation was performed with a different anti-HA antibody (HA-7, 12 μg/IP, Sigma). Briefly, 6-week-old mice were housed in the dark for two weeks before being exposed to light for 0, 1, 3, or 7.5 hr, whereupon the visual cortex was dissected and flash frozen in liquid nitrogen. Visual cortices from three individual animals were pooled for each biological replicate, and three biological replicates were performed. Equal amounts of RNA from the IP and input fractions were amplified with the Ovation RNA Amplification System V2 (NuGEN, San Carlos, CA) and quantitative RT-PCR was performed as described above.

Relative expression levels were determined in every experiment by normalizing the Ct-values to those of beta-Actin (*ActB*) from the 0 hr input using the ΔΔ Ct method. To determine the fold-enrichment (IP/Input), the actin-normalized expression levels for every time point of every biological replicate were averaged, and the grand averages from the IP and Input were divided to find the IP/Input ratio. To calculate fold-induction for each biological replicate, each time point was divided by the maximal value occurring in that biological replicate, such that the maximal value was set to 1 in each biological replicate. The mean and standard error were calculated at each time point from these normalized values. Due to the biological and technical variability inherent in this assay, it is not readily amenable to standard statistical analysis. Instead, transcripts were scored as reliably induced by sensory experience at a given time point on the basis of 2 criteria: 1) the mean value of the time point should be increased by 30% or more over the mean value of the 0h time point, and 2) at least 2 out of the 3 biological replicates at the given time point should be greater than their corresponding 0h time points.

Image Intensity Measurements

For quantification of Narp immunostaining intensity measurements, WT or cKO brains were stained with antibodies directed against Narp and NeuN, and imaged in a blinded manner. Brain sections were imaged on a Zeiss LSM5 Pascal confocal microscope using a 63x objective at 1024 x1024 pixel resolution. For each experiment, all images were acquired with identical settings for laser power, detector gain, and amplifier offset with a pinhole diameter equivalent to one Airy unit for the 633 nm laser; pinhole diameters for the 543 nm and the 488 nm laser were set such that the optical slice thickness was conserved, but they were not changed during the experiment. Laser power and detector gain were set such that pixel intensities remained within the dynamic range. Images were acquired as a Z-stack (8-10 optical sections, 0.75 μm step size). Maximum intensity projections were created from Z-stacks and analyzed using ImageJ and MATLAB.

Images were analyzed blinded; for each image, a threshold was manually determined for NeuN staining, and the somata of tdTomato-positive SST neurons were traced using ImageJ. No threshold was applied to the Narp channel; based on secondary antibody control slides, background fluorescence was found to be a negligible percentage of total signal. Using a custom MATLAB script, the average intensity of the Narp channel was analyzed. This script calculated the average intensity of the pixels of the Narp channel in the area defined by each traced SST neuron in the image. It then determined the average pixel intensity of the Narp channel that overlapped with NeuN; however, pixels that overlapped both with NeuN and traced SST neurons were excluded. The reported data is derived from 3 cKO and 2 WT animals, with at least 15 images per animal taken across multiple brain sections. Intensity data was normalized to the mean of the WT on the same slide, and significance was determined based on the pooled normalized values using a Mann-Whitney U-Test in MATLAB.

Animal Husbandry and Colony Management

Npas4 knockout and conditional knockout mice were generated in the Greenberg lab by Yingxi Lin (Lin et al., 2008). Ai9 Rosa26:: tdTomato reporter mice (Madisen et al., 2010), Emx1-Cre (Gorski et al., 2002), Dlx5/6-Cre (Stenman et al., 2003), PV-Cre (Hippenmeyer et al., 2005), Gad2-Cre, SST-Cre, VIP-Cre (Taniguchi et al., 2011) and RiboTag mice (Sanz et al., 2009) are available from the Jackson Laboratory.

For routine experimentation, animals were genotyped using a PCR-based strategy; PCR primer sequences are available upon request. For most experiments, mice heterozygous for the Npas4 conditional allele ($Npas4^{flx/wt}$) and homozygous for SST-Cre (*Sst-IRES-Cre*) were crossed to mice heterozygous for the Npas4 conditional allele and homozygous for the tdTomato reporter allele (*Rosa-LSL-tdTomato*). Resulting littermates all had one copy of the SST-Cre transgene and the tdTomato Cre-reporter and yielded $Npas4^{wt/wt}$ and $Npas4^{flx/flx}$ littermates for experimentation. The use of animals was approved by the Animal Care and Use Committee of Harvard Medical School.

SUPPLEMENTAL REFERENCES

Clements, J.D., and Bekkers, J.M. (1997). Detection of spontaneous synaptic events with an optimally scaled template. Biophys. J. *73*, 220–229.

Bolstad, B.M., Irizarry, R.A., Åstrand, M., and Speed, T.P. (2003). A comparison of normalization methods for high density oligonucleotide array data based on variance and bias. Bioinformatics *19*, 185–193.

Bortone, D., and Polleux, F. (2009). KCC2 expression promotes the termination of cortical interneuron migration in a voltage-sensitive calcium-dependent manner. Neuron *62*, 53–71.

Ebert, D.H., Gabel, H.W., Robinson, N.D., Kastan, N.R., Hu, L.S., Cohen, S., Navarro, A.J., Lyst, M.J., Ekiert, R., Bird, A.P., and Greenberg, M.E. (2013). Activity-dependent phosphorylation of MeCP2 threonine 308 regulates interaction with NCoR. Nature *499*, 341–345.

Flavell, S.W., Kim, T.-K., Gray, J.M., Harmin, D.A., Hemberg, M., Hong, E.J., Markenscoff-Papadimitriou, E., Bear, D.M., and Greenberg, M.E. (2008). Genome-wide analysis of MEF2 transcriptional program reveals synaptic target genes and neuronal activity-dependent polyadenylation site selection. Neuron *60*, 1022–1038.

Gorski, J.A., Talley, T., Qiu, M., Puelles, L., Rubenstein, J.L.R., and Jones, K.R. (2002). Cortical excitatory neurons and glia, but not GABAergic neurons, are produced in the Emx1-expressing lineage. J. Neurosci. *22*, 6309–6314.

Hippenmeyer, S., Vrieseling, E., Sigrist, M., Portmann, T., Laengle, C., Ladle, D.R., and Arber, S. (2005). A developmental switch in the response of DRG neurons to ETS transcription factor signaling. PLoS Biol. *3*, e159.

Livak, K.J., and Schmittgen, T.D. (2001). Analysis of relative gene expression data using real-time quantitative PCR and the 2(-Δ Δ C(T)) Method. Methods *25*, 402–408.

Madisen, L., Zwingman, T.A., Sunkin, S.M., Oh, S.W., Zariwala, H.A., Gu, H., Ng, L.L., Palmiter, R.D., Hawrylycz, M.J., Jones, A.R., et al. (2010). A robust and high-throughput Cre reporting and characterization system for the whole mouse brain. Nat. Neurosci. *13*, 133–140.

Polleux, F., and Ghosh, A. (2002). The slice overlay assay: a versatile tool to study the influence of extracellular signals on neuronal development. Sci. STKE *2002*, pl9–pl9.

Stenman, J., Toresson, H., and Campbell, K. (2003). Identification of two distinct progenitor populations in the lateral ganglionic eminence: implications for striatal and olfactory bulb neurogenesis. J. Neurosci. *23*, 167–174.

Taniguchi, H., He, M., Wu, P., Kim, S., Paik, R., Sugino, K., Kvitsiani, D., Fu, Y., Lu, J., Lin, Y., et al. (2011). A resource of Cre driver lines for genetic targeting of GABAergic neurons in cerebral cortex. Neuron *71*, 995–1013.

Tao, X., Finkbeiner, S., Arnold, D.B., Shaywitz, A.J., and Greenberg, M.E. (1998). Ca2+ influx regulates BDNF transcription by a CREB family transcription factor-dependent mechanism. Neuron *20*, 709–726.

Tiscornia, G., Singer, O., and Verma, I.M. (2006). Production and purification of lentiviral vectors. Nat. Protoc. *1*, 241–245.

Xia, Z., Dudek, H., Miranti, C.K., and Greenberg, M.E. (1996). Calcium influx via the NMDA receptor induces immediate early gene transcription by a MAP kinase/ERK-dependent mechanism. J. Neurosci. *16*, 5425–5436.

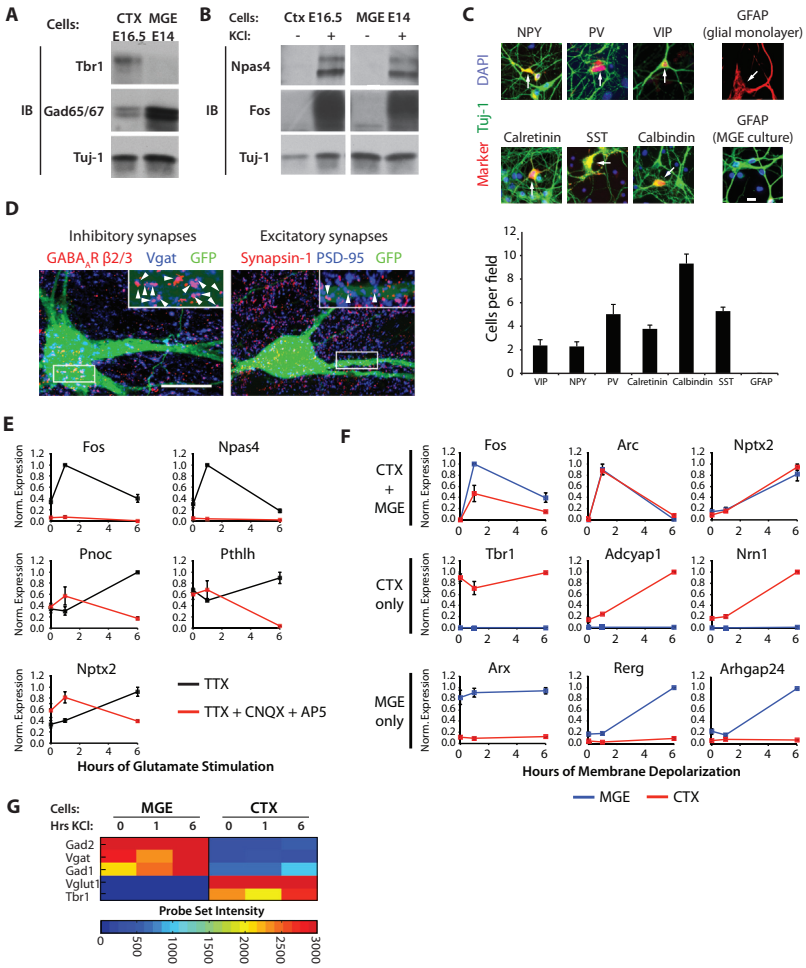

Figure S1. Neuronal Culture Systems to Assay Cell-Type-Specific Inducible Transcriptional Programs in Inhibitory and Excitatory Neurons, Related to Figure 1

(A) Western blot analysis of marker proteins Tbr1 (expressed only in excitatory neurons) and Gad65/67 (expressed only in inhibitory neurons) in age-matched MGE (E14 embryos, DIV9) and mixed cortical (E16.5 embryos, DIV7) cultures.

(B) Western blot analysis of Npas4 and Fos protein in lysates of age-matched MGE (DIV9) and mixed cortical cultures (DIV7) silenced overnight with TTX and AP-5 and depolarized with 55 mM KCl for 0 (-) or 2 hr (+).

(C) MGE-derived cultures contain multiple inhibitory neuron subtypes. Top, example images of immunostaining of DIV10 MGE-derived cultures with antibodies directed against markers of inhibitory neuron subtypes (Red), and Tuj-1 (green), as well as DAPI (blue, scale bar = 20 μm). Bottom, bar graph showing the prevalence of different types of markers (SST, Calbindin, Calretinin, and GFAP were evaluated at DIV10; NPY, PV, and VIP were evaluated at DIV21, as their expression turns on later in development) (Arrows indicate cells expressing the respective marker).

(D) Cultured MGE-derived neurons form synapses. Left, MGE-derived cultures were sparsely transfected with GFP to visualize neuronal processes, fixed at DIV14 and immunostained with antibodies directed against specific markers for inhibitory synapses Vgat (blue) and GABA$_A$Rβ2/3 (red). Right, MGE cultures immunostained with antibodies directed against specific markers of excitatory synapses, PSD-95 (blue) and Synapsin-1 (red). Arrowheads in magnified inlets indicate synapses. (Scale bar = 20 μm).

(E) Glutamate induces gene expression in MGE-derived neurons. Quantitative RT-PCR on RNA isolated from DIV10 MGE cultures stimulated with 10 μM glutamate for 0, 1 or 6 hr in the presence of TTX (black) or TTX, CNQX, and AP-5 (red) for genes that are induced also by membrane depolarization: early-response genes (induced in both MGE and CTX: *Npas4*, *Fos*) and late-response genes (induced only in MGE but not CTX: *Pthlh*, *Pnoc*; induced in both MGE and CTX: *Nptx2*). Data are normalized to the maximal value in the experiment and represent the mean ± SEM of 3 bioreps.

(F) Validation of microarray analysis by qPCR. Quantitative RT-PCR analysis to validate microarray results was performed on RNA isolated from DIV9 MGE (blue) and CTX cultures (red) silenced overnight with TTX and AP-5 and membrane depolarized with 55 mM KCl for 0, 1, or 6 hr. Quantitative RT-PCR analysis was performed for genes that were induced by activity in both cultures (*Fos*, *Nptx2*, and *Arc*, top row), genes that were expressed specifically in CTX cultures (Middle row: *Tbr1* – specific, not regulated, *Adcyap1*, and *Nrn1* – specific and regulated), or genes specifically expressed in MGE cultures (*Arx* – specific, not regulated, *Rerg*, and *Arhgap24* – specific, regulated). Expression values are normalized to the maximal value in the experiment, and data represent the mean ± SEM of 3 bioreps.

(G) Controls for the cell type specificity of the samples analyzed by microarray. Heatmap showing probe set intensity of known cell-type-specific genes in each experimental condition. Probe set intensities are the mean values from two independent biological replicates.

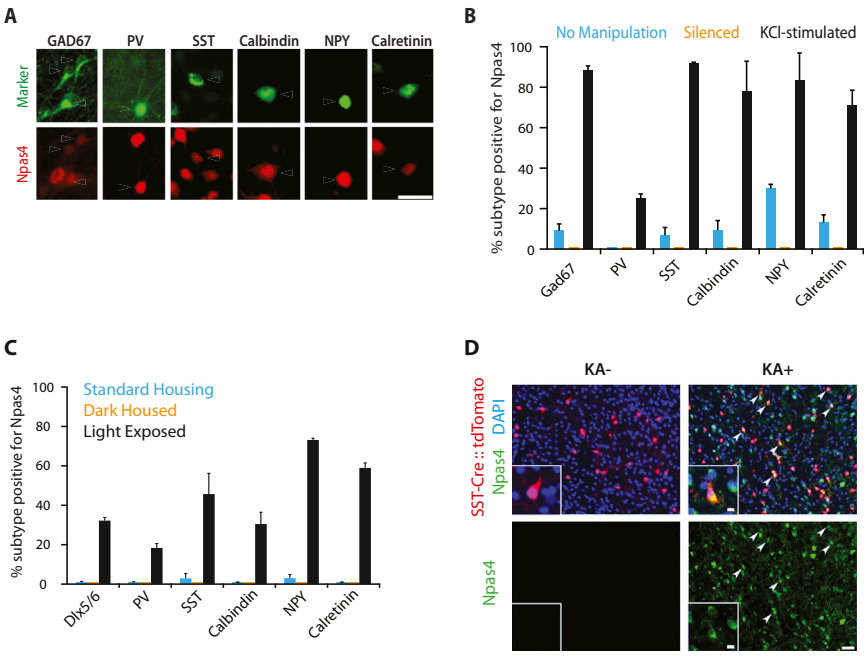

Figure S2. Npas4 Is Induced in Inhibitory Neurons by Membrane Depolarization, Related to Figure 2

(A–C) Npas4 is induced by neuronal activity in multiple inhibitory neuron subtypes. A) Representative images of DIV14 mixed cortical cultures silenced overnight with TTX and AP-5, membrane depolarized for 2 hours by 55 mM extracellular KCl, and immunolabeled with antibodies directed against Npas4 (red) and markers of different inhibitory neuron subtypes (green) (scale bar = 10 μm).

(A) Representative images of DIV14 mixed cortical cultures silenced overnight with TTX and AP-5, membrane depolarized for 2 hr by 55 mM extracellular KCl, and immunolabeled with antibodies directed against Npas4 (red) and markers of different inhibitory neuron subtypes (green, cell bodies indicated by arrowheads, scale bar = 10 μm).

(B) Quantification of the percentage of Npas4-positive cells in specific inhibitory neuron subtypes in unperturbed DIV14 mixed cortical cultures (blue), after overnight treatment with TTX and AP-5 (orange), or after overnight treatment with TTX and AP-5 and two hours of membrane depolarization with 55 mM extracellular KCl (black). Data represent the mean + SEM of 3 bioreps.

(C) Quantification of the percentage of Npas4-positive cells in specific inhibitory neuron subtypes in the visual cortex of P24 wild-type mice raised in standard housing (blue), dark housed for four days (P20-24, orange), or dark housed and subsequently exposed to light for 2.5 hr (black). Inhibitory neuron subtypes were labeled using antibodies directed against proteins that mark different types of inhibitory neurons. Data represent the mean + SEM of 3 bioreps.

(D) Kainate stimulation induces expression of Npas4 in SST neurons in P11 mice. Example images of immunostaining for Npas4 (green) in the brain of P11 mice heterozygous for SST-Cre and a Cre-dependent tdTomato reporter allele labeling SST neurons (red) before kainate (KA-, left) or two hours after administration of kainate (KA+, right) (3 mg/kg kainate were injected intraperitoneally). SST neurons that stained positive for Npas4 are labeled with white arrowheads (scale bar = 20 μm, 5 μm on inset).

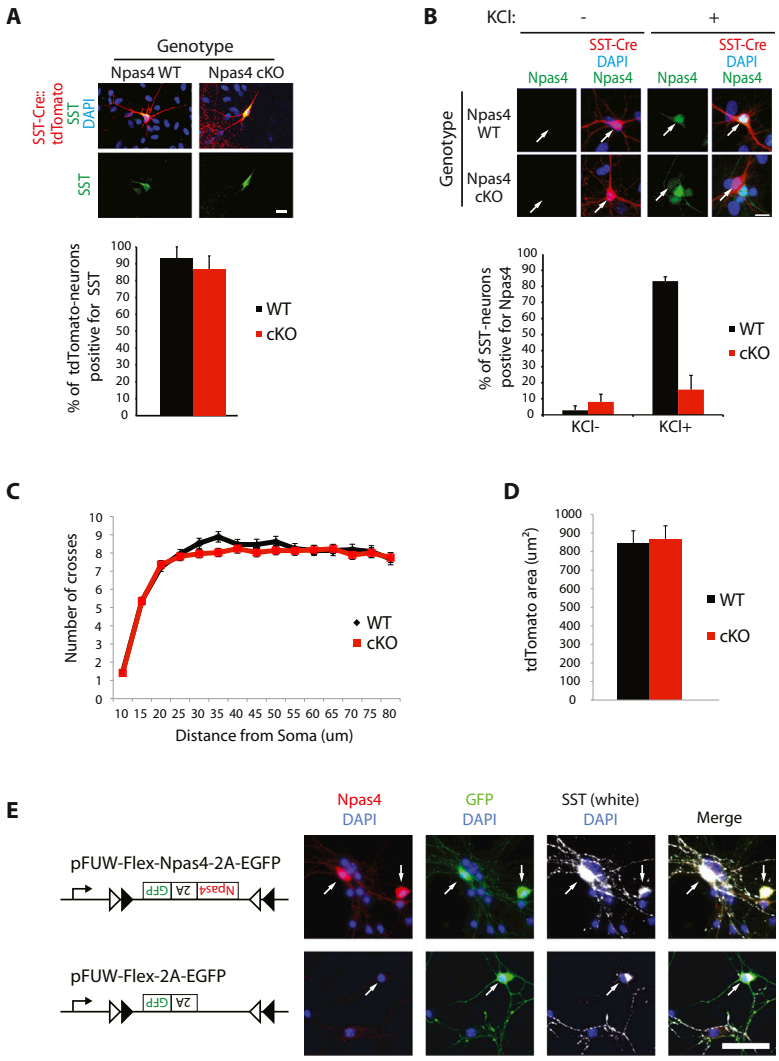

Figure S3. Deletion and Overexpression of Npas4 in SST Neurons in Mixed Cortical Cultures, Related to Figure 3

(A–D) Deletion of Npas4 in SST neurons in mixed cortical cultures.

(A) SST-Cre labels SST-neurons efficiently in vitro. Top, representative images of DIV14 mixed cortical cultures made from Npas4 WT or cKO littermate embryos in which expression of SST-Cre is indicated by a Cre-dependent tdTomato allele (red). Cultures were stained with antibodies against somatostatin (green, scale bar = 10 μm). Bottom, graph showing the percentage of tdTomato-labeled SST neurons that stain positive for SST protein in WT (black) or cKO (red) cultures. Data represent the mean + SEM of 3 bioreps.

(B) SST-Cre efficiently excises the floxed Npas4 cKO allele in SST neurons in culture. Top, example images of Npas4 WT (top) or Npas4 cKO (bottom) DIV14 mixed cortical cultures silenced overnight (-) or silenced overnight and subsequently membrane depolarized for 2 hr with 55 mM KCl (+) immunolabeled with antibodies directed against Npas4 (green). tdTomato-labeled SST neurons (red, arrows) only stain positive for Npas4 in WT cultures upon membrane depolarization (scale bar = 10 μm). Bottom, graph showing the percentage of SST neurons that stain positive for Npas4 before or after membrane depolarization. Data represent the mean + SEM of 3 bioreps.

(C) Selective deletion of Npas4 does not significantly alter the complexity of proximal dendrites in SST neurons in mixed cortical cultures. Sholl analysis of WT or Npas4 cKO tdTomato-labeled SST neurons in DIV14 cortical cultures. Data represent the mean ± SEM of 3 bioreps.

(D) Selective deletion of Npas4 does not significantly alter the total dendritic area of SST neurons in mixed cortical cultures. Quantification of the total dendritic area of tdTomato-labeled SST interneurons in DIV14 E16.5 cortical cultures prepared from Npas4 WT or cKO littermate embryos. Data represent the mean + SEM of 3 bioreps.

(E) Cre-dependent overexpression of Npas4 in SST neurons in mixed cortical cultures. Left, lentiviral constructs expressing in a Cre-dependent manner either Npas4 and GFP (pFUW-Flex-Npas4-2A-EGFP) or of GFP alone (pFUW-Flex-2A-EGFP). Right, DIV8 mixed cortical cultures prepared from SST-Cre E16.5 embryos infected at DIV4 with either pFUW-Flex-Npas4-2A-EGFP (top row) or pFUW-Flex-2A-EGFP (bottom row) and stained for Npas4 (red), GFP (green), somatostatin (SST) (white) and DAPI (dark-blue) (arrows = infected neurons cells) (scale bar = 50 μm).

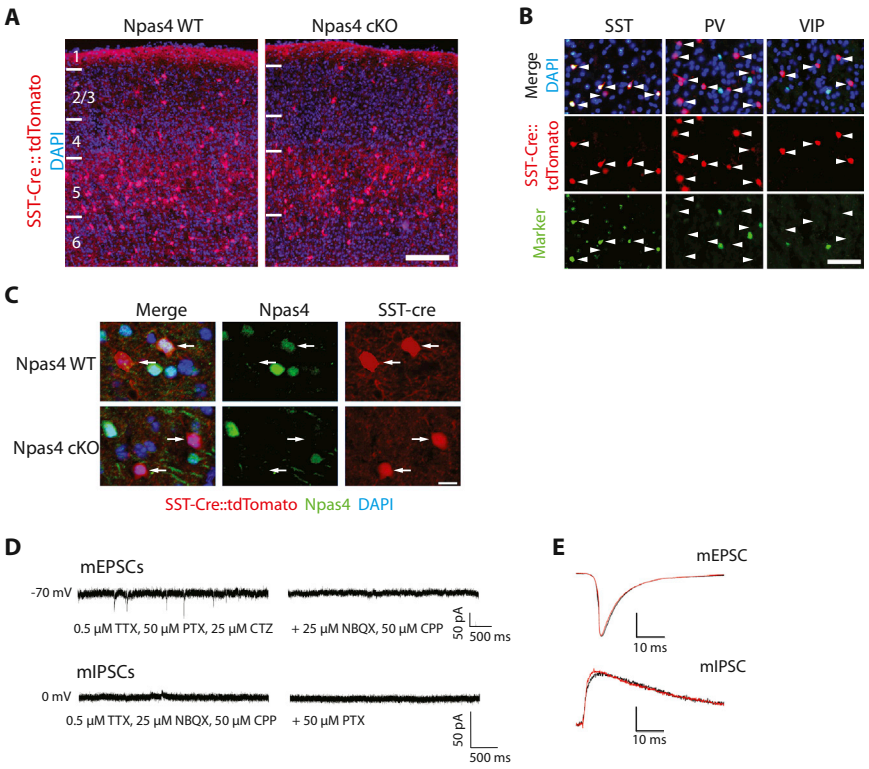

Figure S4. Selective Deletion of Npas4 from SST Neurons In Vivo, Related to Figure 4

(A) Example images of 20 μm coronal sections through the visual cortex of P10-12 Npas4 WT or cKO (lacking Npas4 specifically in SST neurons) mice. DAPI (blue) marks nuclei and tdTomato (red) reports SST-Cre expression to label SST-positive inhibitory neurons, cortical layers are indicated on the left (scale bar = 250 μm).

(B) SST-Cre is expressed specifically in SST neurons. Example images from visual cortex of P24 mice heterozygous for SST-Cre and the tdTomato Cre reporter (red) stained with antibodies against Somatostatin (SST), Parvalbumin (PV), or Vasointestinal Peptide (VIP) labeled in green. SST-Cre-labeled neurons (arrows) stain positive for SST, but not PV or VIP (scale bar = 50 μm).

(C) SST-Cre excises the floxed Npas4 allele in SST neurons in the brain. P24 Npas4 WT or cKO (lacking Npas4 specifically in SST neurons) animals were dark housed for four days starting at P20, exposed to light for 2 hr at P24, and immunostained with antibodies against Npas4 (green). Npas4 is expressed in approximately half of SST neurons (red) in WT visual cortex, but is absent from SST neurons in the visual cortex of Npas4 cKO mice (arrow, scale bar = 5 μm).

(D) Pharmacological blockade shows specificity of miniature currents. Top, example trace of mEPSCs in SST neurons held at −70 mV; events were blocked by application of 25 μM NBQX and 50 μM CPP. Bottom, example trace of mIPSCs in SST neurons held at 0 mV, and events were blocked by application of 50 μM picrotoxin (PTX). (Scale bars for all traces are 50 pA and 500 ms, n = 2 cells for each pharmacological blockade).

(E) Normalized average traces from wild-type (black) or Npas4 cKO (red) SST neurons for mEPSCs (top), and mIPSCs (bottom). (scale bar = 10 ms).

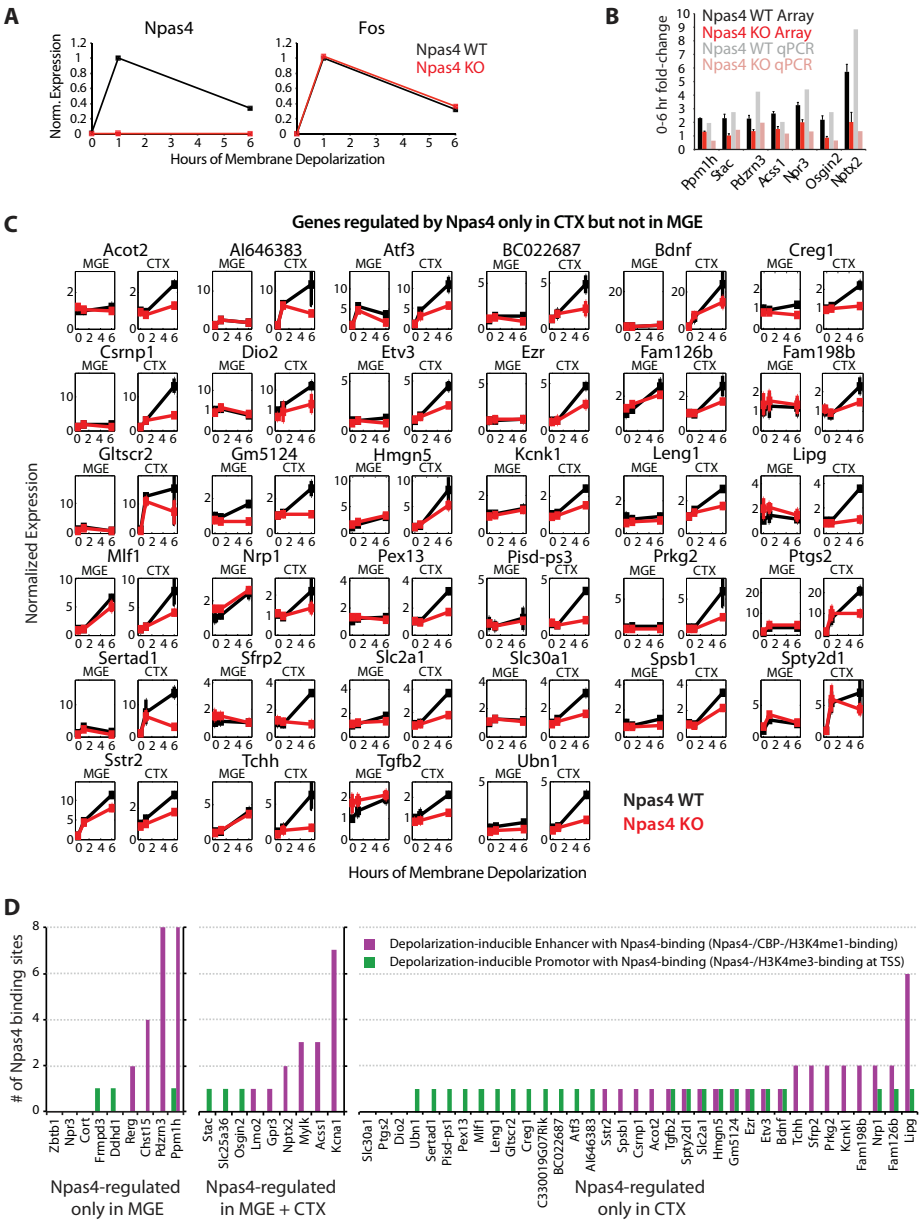

Figure S5. Cell Type Specificity of Npas4 MGE Target Genes, Related to Figure 5

(A) *Npas4* mRNA is absent in Npas4 KO MGE and CTX cultures. Quantitative RT-PCR for *Npas4* from DIV10 MGE and CTX cultures prepared from WT (black) or Npas4 KO (red) littermate embryos. Data are normalized to the maximal value in the experiment.

(B) Quantitative RT-PCR experiments confirm the results of microarray-based analysis of the Npas4-regulated transcriptional program in inhibitory neurons. RNA was isolated from an independent biological replicate of DIV9 MGE cultures prepared from Npas4 WT or KO littermate embryos that were silenced with TTX and AP-5 overnight and then membrane depolarized with 55 mM extracellular KCl for 0 or 6 hours. Quantitative RT-PCR analysis was performed on seven Npas4-regulated genes, and for each gene, the 0-6 hour fold-induction from Npas4 WT (grey) or Npas4 KO (pink) cultures were directly compared to the 0-6 fold-induction of the array signal from Npas4 WT (black) or KO (red) MGE cultures. Microarray data represent the mean + SEM of 2 bioreps.

(C) Microarray-based line plots of genes regulated by Npas4 specifically in CTX neurons. Line plots show normalized expression plotted versus time of membrane depolarization (hours). Data are normalized to the WT CTX 0h sample (WT = black, KO = red) and represent mean + SEM of 2 bioreps.

(D) Npas4 target genes in MGE and CTX are associated with Npas4-bound gene regulatory regions. Bar graph shows the number of inducible Npas4 binding sites at the genomic locus of each Npas4-regulated gene either at enhancer elements (purple, defined by inducible binding of CBP and the presence of H3K4me1) that are located within 50 kb upstream of the transcriptional start site (TSS) or within the gene's intronic regions, and/or at the promoter (green, defined by the presence of H3K4me3 at the mRNA TSS).

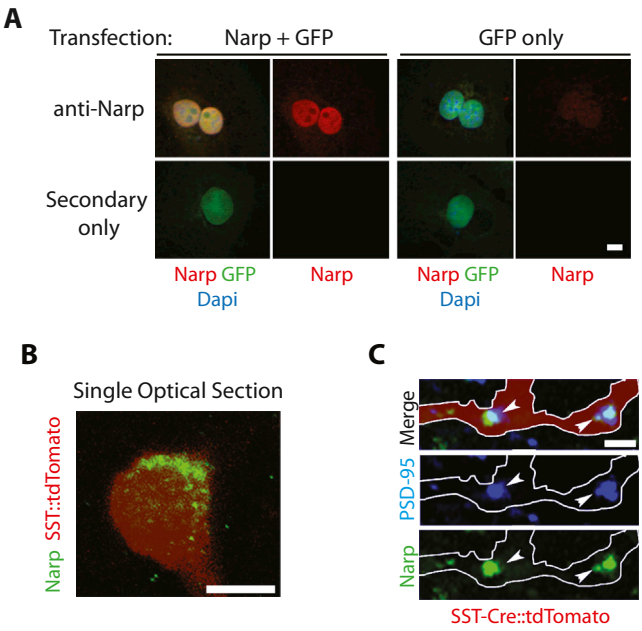

Figure S6. Narp Is Expressed at Excitatory Synapses onto SST Neurons, Related to Figure 6

(A) Antibodies against Narp specifically recognize heterologously expressed Narp. Cos-7 cells were co-transfected with expression vectors containing *Nptx2* cDNA (Narp) and GFP (left) or GFP alone (green, right) and stained with an antibody directed against Narp (red, top) or only with secondary antibodies (bottom) to determine Narp antibody specificity. The Narp antibody specifically recognizes the gene product encoded by the *Nptx2* cDNA.

(B) Narp is expressed in SST neurons in the visual cortex in vivo. Single confocal optical section through a SST neuron (red) from a WT P11 brain stained with antibodies directed against Narp (green). This representative image shows perisomatic localization of Narp in cortical SST neurons consistent with Narp synthesis in those cells (scale bar = 10 μm).

(C) Narp is localized at excitatory synapses onto SST neurons in the visual cortex in vivo. Brain sections from P11 WT mice with tdTomato-labeled SST neurons (red) were stained with antibodies against PSD-95 (blue) and Narp (green). This high magnification maximal intensity projection shows that Narp puncta can be observed colocalizing with PSD-95 puncta (arrowheads) on SST neuron dendrites (white outline, scale bar = 1 μm).